Molecular Electronic Junctions

Richard L. McCreery*

Department of Chemistry, The Ohio State University, 100 West 18th Avenue, Columbus, Ohio 43210-1185

Received March 21, 2004. Revised Manuscript Received June 18, 2004

A review with 228 references on experimental investigation of conductor/molecule/metal molecular electronic junctions is presented. Devices based on covalent and Langmuir−Blodgett bonding of single molecules or molecular monolayers to conducting substrates are reviewed, as characterized by scanning probe microscopy and microelectronic techniques. Phenomena observed to date include molecular rectification, conductance switching, and nonlinear current/voltage behavior. Prospects and problems for the application of molecular junctions to the more general area of molecular electronics are discussed.

1. Introduction and Scope

The term "molecular junction" came into use relatively recently, but has conceptual roots which span at least the latter half of the 20th century. Several diverse areas of chemistry and physics provide the context for a discussion of molecular junctions, and will be reviewed briefly here to serve as an introduction. The theme which is common to all is electron transport through organic molecules, often involving metallic or semiconducting solids with which the molecules are in electrical contact.[1−5] First, organic thin film devices are qualitatively similar to molecular junctions, in that they consist of an organic layer between two or more conducting or semiconducting solids. Examples include classical capacitors with an organic dielectric layer, organic light-emitting diodes, and conducting polymers. While the literature on such devices is extensive, they are generally not considered molecular junctions because the organic film is much thicker than the molecular dimensions, and is generally disordered. Second, electron transfer in donor−bridge−acceptor (DBA) molecules (Figure 1a) has been actively investigated, in part to determine which aspects of bridge structure control the electron-transfer (ET) rate.[6−12] Third, closely related electrochemical experiments, in which the donor or acceptor is replaced by a conducting solid (Figure 1b), also seek to reveal how the ET rate depends on the "bridge" structure.[13−21] In addition, electron transfer in thin films of polymers containing redox centers has been investigated with respect to transport of both electrons and ions in the associated electrolyte.[22−27] Fourth, significant progress has been made in theoretically modeling ET through molecules[3,4,22,28−36] since the idea of a molecular rectifier was proposed by Aviram and Ratner in 1974.[37] Related theory and experiments on bulk organic conductors provide important analogues for ET in molecular junctions.[38−44]

Many of the concepts and results of these diverse investigations are directly related to molecular junction behavior, and will be cited as appropriate. However, several fundamental aspects of junction electronic behavior are not encountered in bulk organic films, DBA molecules, or electrochemical experiments. Although there is not yet a widely accepted definition of the term "molecular junction", some of these special characteristics serve to define their nature, and they are discussed in more detail below. For now, let us assume that a molecular junction incorporates one or more molecules in electrical contact with two (usually) conductors, such that electrons are transmitted through the molecule(s), as shown schematically in Figure 1c. In this review bulk organic materials, DBA molecules, or electrochemical kinetics will not be discussed in detail, except as they bear on molecular junction behavior. Although carbon nanotubes might be considered together with more traditional molecules, space prevents discussion of the many interesting electronic effects observed in nanotube devices.[42,45−52] In all cases, the discussion is limited to junctions with molecular layers with thickness no more than a few times the dimensions of a monomeric molecule. In addition, the review emphasizes experimental results rather than theoretical modeling. Overall, the principal objectives of investigations of molecular junctions are both fundamental and practical: elucidation of the factors which control ET through single

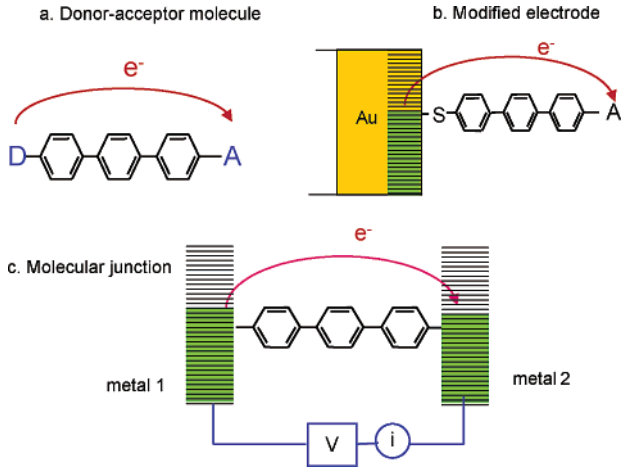

Figure 1. Electron transfer in donor−acceptor molecules (a), modified electrodes in solution (b), and molecular junctions (c). In all three cases, a key issue is the effect of bridge structure on electron-transfer kinetics.

* Phone: (614) 292-2021. E-mail: mccreery.2@osu.edu.

10.1021/cm049517q CCC: $27.50
Published on Web 08/11/2004

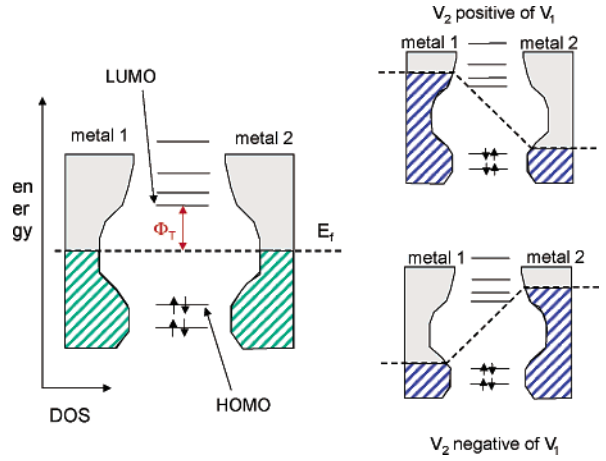

Figure 2. Schematic energy levels of a metal/molecule/metal molecular junction at zero bias (left) and with an imposed voltage (right). The curved portion of the metal contacts represents the density of electronic states in the metal, and E_f is the Fermi level. The green hashed region represents the filled orbitals when $V = 0$, and blue regions are filled orbitals when a bias is applied. The dashed lines in the right drawing represent the imposed electric field, and Φ_T is the tunneling barrier at zero bias.

molecules or molecular monolayers, and possible incorporation of molecular properties into electronic circuits.

2. Elements of a Molecular Junction

A complete understanding of a molecular junction would view the entire structure as one electronic system, to consider perturbations of each component by electronic interactions with others. To make the problem tractable, the junction is usually broken down into several components, often separated by one or more energy barriers. The conductors to which the molecules of interest are bonded are often called "contacts", and are characterized by a distribution of electronic energy levels and associated densities of electronic states (DOS). Metals have a high, generally uniform DOS, while semiconductors have conduction bands, valence bands, and band gaps. These levels may be partially or fully occupied, as predicted by the Fermi distribution function. Application of a voltage across the junction causes the electrons in the contacts to redistribute, with the negative electrode having a larger fraction of filled orbitals. A schematic representation of energy levels and densities of states of the contacts is shown in Figure 2.

The connection between contacts and molecule(s) has received significant attention, due to its importance as the interface between molecular and conventional electronics. If molecular electronic devices are ever to be interfaced with conventional power sources, displays, sensors, etc., we will need "alligator clips" of some sort to establish electronic contact. A major consideration of such an alligator clip is the energy barrier an electron must cross (or tunnel through) to be transmitted from the contact to the molecule.[31−33,53−55] If this barrier is very large, the molecule and conductor are effectively isolated and do not interact electronically. The opposite limit is often called an "ohmic contact", in which the electron may move freely between molecule and conductor and the electronic coupling between the molecule and contact is strong. Specific examples of contact/molecule interfaces are discussed at some length below, but they cover a wide range between "ohmic" and "insulating".

Table 1. Conduction Mechanisms in Metal/Molecule/Metal Thin Film Junctions[a]

	temperature (T) dependence	voltage (V) dependence	monolayer thickness (d) dependence
coherent tunneling, "superexchange"	none	linear (low V)	$\exp(-\beta d)$
Incoherent, diffusive tunneling "tight binding model"	none (see the text)	linear (low V)	$\exp(-cd)$
"hopping" (i.e., "ohmic")	$\exp(-a/T)$	linear (low V)	d^{-1}
Poole−Frenkel effect ("traps")	$\exp(-a/T)$	$\exp(bV^{1/2})$	$\exp(-cd^{1/2})$
thermionic (Schottky) emission	$\exp(-a/T)$	$\exp(bV^{1/2})$	$\exp(-cd^{1/2})$
field emission (high E field, "Fowler−Nordheim")	none	$V^2 \exp(-b/V)$	$\exp(-cd)$

[a] a, b, and c denote constants which are independent of temperature, voltage, and thickness, respectively. Compiled from refs 2, 3, 30, 53, 57, 58, 76, and 85, using a format similar to that of Sze.[85]

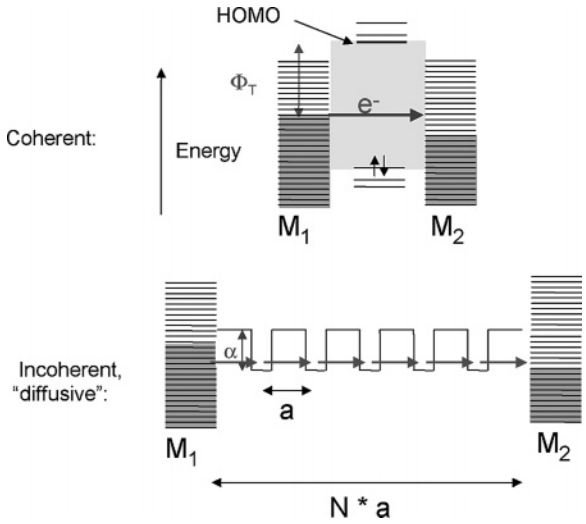

Figure 3. Schematic energy level diagrams for coherent and diffusive tunneling. Φ_T is the barrier for coherent tunneling, α is the potential well depth of N sites spaced apart by a distance a. M_1 and M_2 are the metallic contacts. See ref 77 for a detailed description.

2.1. Electron Transport in Molecules. As noted earlier, the ET mechanisms in single molecules have been investigated in some detail, mainly in the context of donor−bridge−acceptor molecules studied by spectroscopic techniques. A variety of ET mechanisms have been considered which depend on molecular size and structure, as well as temperature and the magnitude of the free energy difference between donor and acceptor. Table 1 lists a few mechanisms reported for ET in molecules, along with more classical processes reported for bulk materials. Several of these mechanisms are particularly relevant to molecular junctions, and a brief elaboration of Table 1 is warranted. More complete discussions are available in several reviews.[4,5,7,56]

2.1.1. Coherent Tunneling. Classical, or coherent, tunneling dictated by quantum mechanics is based on the probability of an electron traversing a barrier of some thickness and barrier height, and maintains the phase of the electron (Figure 3). The rate of coherent tunneling decreases exponentially with the thickness of

the barrier, and is given in its simplest form by the Simmons relation, eq 1,[57,58] where J = current density, A/cm^2, q = electron charge, V = applied voltage, h = Plank's constant, m = electron mass, Φ = barrier height, and d = barrier thickness.

$$J = \frac{q^2V}{h^2d}(2m\Phi)^{1/2} \exp\left[\frac{-4\pi d}{h}(2m\Phi)^{1/2}\right] \quad (1)$$

Equation 1 shows only the linear term for a rectangular tunneling barrier, but it does show the exponential dependence on d. In the case of a molecular junction such as that of Figure 2, d is the distance between conductors and Φ_T is the tunneling barrier height in joules or electron volts. Equation 1 is often simplified to a form useful for comparison to experiment, eq 2, where B is a constant and β has units of inverse angstroms or inverse nanometers. By comparison to eq 1, we note that β is proportional to the square root of the barrier height.

$$J = Be^{-\beta d} \quad (2)$$

Although observed tunneling rates in molecular junctions often depend exponentially on the junction thickness, the observed value of β is at times surprising. For a vacuum gap between two metals with work functions of 5.0 eV, eq 1 predicts $\beta = 2.3$ Å^{-1}, while observed β values in molecular junctions[59−61] are often near 1.0 Å^{-1}. This difference is significant, since the tunneling rate depends exponentially on β and d. For example, an increase in d from 5 to 10 Å should decrease the ET rate from coherent tunneling by a factor of 150 for β = 1.0 Å^{-1}, but by a factor of $\sim 10^5$ for $\beta = 2.3$. Conversely, an observed β of 1.0 yields a barrier height of 0.96 eV according to the Simmons formula. This value is much smaller than the HOMO−LUMO gap of typical junction molecules (5−10 eV), so there must be more to the story than the Simmons model.

A generally accepted explanation for faster than expected tunneling is "superexchange".[11,62−68] Interactions of the electron with the orbitals and electronic structure of the molecule enhance the tunneling rate, making "through bond" tunneling more efficient than "through space" tunneling. However, even a relatively small β of 0.5 Å^{-1} predicts a decrease in the ET rate by a factor of >20000 for a 20 Å molecule, leading to the conclusion that coherent tunneling is effective only for short distances.

Although tunneling, with or without superexchange, should not depend on temperature, the conformation of the molecule does. If molecular vibrations or internal rotations create a geometry with a smaller barrier to tunneling, the tunneling itself will appear to be temperature dependent.[69] Enhanced tunneling as a consequence of conformational changes is an example of an "activated" process which is expected to be temperature dependent, and examples are provided below. As a rule of thumb, coherent tunneling, even assisted by superexchange or conformational changes, is not effective over distances greater than ~25 Å, often less. ET over such distances is usually ascribed to more complex phenomena, such as "diffusive tunneling" or "hopping".

2.1.2. Incoherent, Diffusive Tunneling. A surprising observation of the early 1990s was ET of an electron through ~40 Å of a DNA helix.[65,70−75] Since this distance was too large for coherent tunneling, and DNA was not known to be a "conductor" in the usual sense, another mechanism must be involved. Incoherent tunneling or the "tight binding" model proposes that the electron tunnels coherently along a series of sites, which are characterized by potential wells (Figure 3).[76,77] The residence time of the electron in a potential well is long enough to disturb the phase of the electron, and the process may be viewed as a series of discrete steps. It is "diffusive" because the path of the electron may follow a random walk between sites. However, it is important to recognize that the electron tunnels through the barriers between sites, and the process is not dependent on temperature to a first approximation. In one theoretical treatment, the occupied "sites" are considered to be organic anion radicals, and the barrier to tunneling is related to the reorganization energy between neutral and anion geometries of each site.[78]

2.1.3. Hopping Mechanisms. The term "hopping" usually refers to thermally activated ET which follows a classical Arrhenius relation such as eq 3, where k_{ET}

$$k_{ET} = k_{ET}^{\circ} \exp(-E_a/kT) \quad (3)$$

is the ET rate, E_a is an activation barrier, and k is the Boltzman constant. Like incoherent tunneling, the electron may traverse one or more sites, but the difference between tunneling and hopping is the involvement of nuclear motion.[22,30,79−81] ET does not occur until thermal motion of nuclei results in a favorable molecular geometry. Hopping involves electron motion *over* the barrier (meaning the molecule must rearrange for ET to occur), while tunneling involves ET *through* the barrier (meaning there is a finite probability of finding the electron on the other side of the barrier, without requiring nuclear motion). Since hopping involves a series of transfers between relatively stable sites, it does not exhibit the exponential distance dependence of coherent tunneling, but instead varies as $\sim d^{-1}$. It is also the basis of ohmic conduction, and follows a dependence on driving force predicted by Marcus theory. A comparison of the distance and temperature dependence of coherent tunneling with hopping is shown in Figure 4. The slope of the slanting line for tunneling depends on the tunneling barrier but not on temperature, while the series of lines for hopping are strongly temperature dependent. For a homologous series with varying length (e.g., polyphenylene oligomers), we expect coherent tunneling for small d, but hopping for larger d. For large d, the distance is too great for coherent tunneling, and the electron can propagate more efficiently by a series of "hops".

Although in this review experimental results on molecular junctions are stressed, a theoretical aspect of metal/molecule contacts and electron transport in molecules bears on the brief discussions of tunneling and hopping in the previous three sections. The problem may be approached from the perspective of activated electron transfer associated with Marcus theory and familiar to electrochemists, or from a Landauer approach involving electron transport with limited nuclear motion.[56,66,76,77,82−84] The Marcus approach involves discrete reactants and products (e.g., a neutral species and an anion radical), while the Landauer picture is

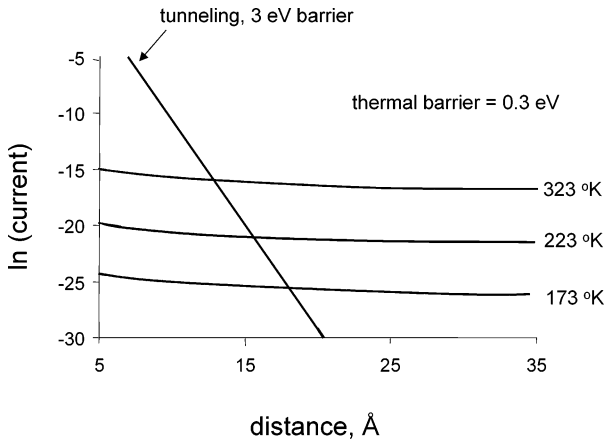

Figure 4. Theoretical comparison of the coherent tunneling current (3 eV barrier height) with the current arising from thermal activation over a 0.3 eV barrier, both as functions of the junction thickness. For the thermal case, the imposed field is assumed to increase the current according to the thermionic mechanism depicted in Figure 5. Note also that tunneling is temperature independent, while the thermal mechanism is strongly T dependent. Note that the current scale is logarithmic. See ref 191 for further discussion.

based on electron tunneling without (necessarily) molecular reorganization. While it is tempting to refer to a Marcus mechanism as activated and temperature dependent, while electron tunneling is neither, there are shades of gray between these two limits. For example, ET in a molecule with several subunits might be viewed as tunneling between a series of potential wells,[77] or as successive electron transfers between radical ion centers.[78] The time an electron resides in various potential wells relative to the time for molecular reorganization is a key parameter in assessing the importance of nuclear motion to electron transport.

2.1.4. Poole–Frankel Effect. Poole–Frankel conduction is related to hopping, and was developed to explain the effect of "traps" in semiconductors.[57,85] A trap in this context is a "Coulombic" site whose potential well depth varies in an electric field. Like Schottky emission (see below), it varies exponentially with the square root of the electric field, but the energy barriers for Poole–Frankel conduction are within the molecule rather than at the molecule/contact interface. Schottky emission and Fowler–Nordheim tunneling are definitely interfacial effects, and are discussed next.

2.1.5. Fowler–Nordheim Tunneling. Also called "field emission", Fowler–Nordheim tunneling refers to an enhanced tunneling rate which occurs in high electric fields. "High" usually means that the applied voltage exceeds the barrier height and is well beyond the linear voltage behavior implied by the Simmons relation. It is nominally independent of temperature, but decreases exponentially with distance, as indicated in Table 1.[57,85]

2.1.6. Schottky Emission. Sometimes referred to as thermionic emission, Schottky emission was investigated originally to explain ET at interfaces of semiconductors with metals or other semiconductors. A Schottky barrier usually arises from partial charge transfer from one phase to another at an interface, generating a "depletion layer", and an electrostatic barrier. As shown in Figure 5, the barrier height is influenced by the local electric field, with the result being a nonlinear dependence of ET on the applied voltage. The Schottky–

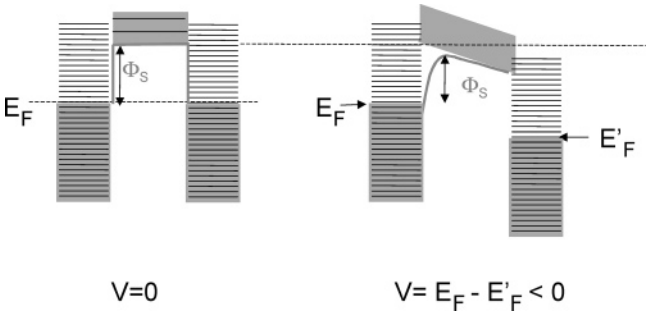

Figure 5. Schottky or thermionic emission over a barrier with height Φ_S. Application of a voltage (right diagram) lowers the barrier height due to the imposed electric field.

Richardson relation (eq 4) has been shown to apply to a variety of semiconductor interfaces,[57,85,86] and has been invoked to explain several molecular junctions, as discussed later. In addition to the variables defined

$$i = AT^2 \exp\left[\frac{-\Phi}{kT}\right] \exp\left[\frac{V^{1/2}q^{3/2}}{2kT\epsilon^{1/2}d^{1/2}}\right] \qquad (4)$$

earlier, eq 4 includes the dielectric constant, ϵ, the Boltzmann constant, k, the Richardson constant, A, and the absolute temperature, T. Note that the ratio V/d equals the applied electric field, and that a plot of $\ln(J)$ vs $V^{1/2}$ should be linear.

2.2. Classifications of Molecular Junctions. Given that molecular junctions as defined here include contacts, contact/molecule interfaces, and molecules, there remains a fairly wide variety of junction structures. These may be subdivided according to fabrication chemistry (Langmuir–Blodgett, self-assembled monolayer (SAM), etc.), basic structure (single or multiple molecules, two or three terminals, etc.), or experimental paradigm (scanning probe microscopy, break junction, nanopore, etc.). Since junction chemistry and experimental paradigms are likely to evolve with time, we will use a classification based on junction structure. The term "single-molecule junction" will be reserved for junctions in which single molecules behave independently and the molecular "layer" of the junction contains a small number of molecules, usually fewer than 10. A "monolayer junction" has many molecules (e.g., 10^3–10^{12}) in a single, oriented monolayer between the conducting contacts. It is important to distinguish monolayer junctions from thin film devices, in which the molecular layer is usually more than 10 nm thick. The latter case may involve a crystalline or disordered molecular layer, such as an organic transistor or conducting polymer. However, the molecular layer in a conventional thin film device is many molecules thick (>10), and its properties approach those of a bulk material. It is useful to note that a monolayer junction may exhibit molecular electronic properties such as rectification and conductance switching, which are distinct from those observed in bulk materials. At least in practical terms, a monolayer junction is intermediate between a single-molecule junction and a disordered or crystalline thin film device. Strictly speaking, a monolayer junction is a thin film device, of course, but the oriented monolayer imports distinct properties not observed in traditional thin film junctions.

Table 2. Examples of Molecular Junctions

substrate	molecule/binding mode	top contact	no. of molecules	section	references
Au	xylyldithiol/SAM	STM	~1[a]	3.1	118
Au	phenylethynyl/SAM	STM	~1	3.1	116, 127, 132,133
Au	alkane/SAM	CP-AFM	1−5	3.1	59, 131, 149
Al/Al_2O_3	porphyrin/adsorption	Pb	~1	3.1	135
graphite	heteropolyacid/adsorption	STM	~1	3.1	139
Au	biphenyl/SAM/BJ[b]	Au	~1	3.2	86, 156
Au	bypyridine, etc./BJ[b]	Au/STM	~1	3.2	125, 158
graphite	porphyrin	STM		4.1	172
Au, Si	porphyrin, ferrocene	Ag[c]	$\sim 10^6$	4.1	106, 160, 166, 168, 171
Au	phenylethynyl/SAM	Ti	~1000	4.2.1	156, 182
Au	dithiol/SAM	Au	~1000	4.2.2	184
Hg, Ag	SAM	Hg	$\sim 10^{11}$	4.2.3	61, 185−188
Al_2O_3, Au	DBA/LB	Au	$\sim 10^{12}$	5.1	87, 88, 91, 199
Al_2O_3	rotaxane/LB	Ti	$\sim 10^6$	5.2	90, 92, 201
Si	olefin/irreversible	STM	~1	6.1	107, 115, 210
C (glassy)	diazonium/irreversible	Hg	$\sim 10^{11}$	6.2.1	190−192
C (glassy)	diazonium/irreversible	Ti	$\sim 10^{11}$	6.2.2	227

[a] "~1" denotes a junction with 1−10 molecules, and in several cases the small number of molecules probed by an SPM tip. [b] Break junction. [c] Electrolyte present; Ag was the counter electrode.

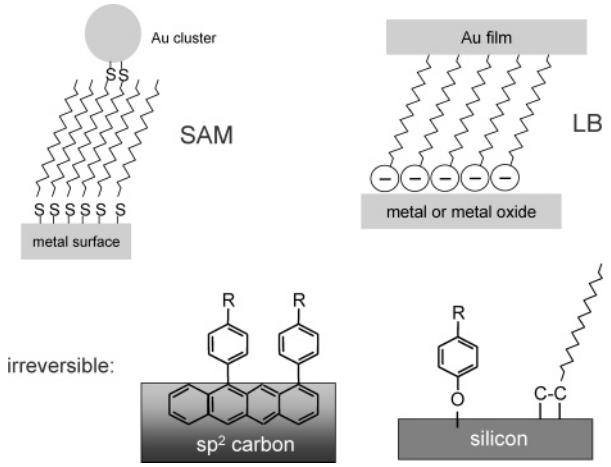

Figure 6. Three junction structures, based on SAMs, LB monolayers, and irreversible bonding to a substrate. In each case, the junction is completed by application of a top contact, possibly with a covalent bond such as that shown for a Au cluster on dithiol SAMs.

The discussion of single-molecule and monolayer junctions will comprise most of the remainder of this review, but some general comments about junction chemistry and paradigms are appropriate at this point. As noted earlier, the nature of the contact/molecule interface is quite important to junction behavior, and it is defined mainly by the "linker chemistry" used to attach the molecules to the contact material. Such chemistry falls into three categories, two of which (SAM and irreversible) are used for both single-molecule and monolayer junctions. These general linker types are shown in Figure 6. The Langmuir−Blodgett (LB) technique uses hydrophobic interactions to orient and assemble a monolayer on the surface of water, and then the film is transferred to a conducting substrate.[87−92] The interaction between molecule and contact is generally a weak electrostatic interaction, similar to the physisorption which occurs at many solid/gas and solid/liquid interfaces. SAMs are most often based on chemisorption of thiols to a metal contact, often Au, Ag, or Hg.[61,93−102] The 40 kcal/mol Au−S bond forms reversibly, so that the monolayer can anneal by repeated desorption and adsorption to result in a close-packed structure with a regular lateral orientation of monolayer molecules. In particular, the alkanethiol SAM on Au has been characterized in detail, and is the basis of many electrochemical studies of ET through molecules.[20,93,103,104] The third class of linkers depicted in Figure 6 is used in a minority of applications, and involves formation of an irreversible molecule−surface bond. The Si−C, Si−O−C, and C−C bonds in these systems are generally quite strong (~80−100 kcal/mol), so surface rearrangement after chemisorption is unlikely.[105−115] In a few cases, the adsorbate layer is ordered due to the initial geometry of the Si surface,[107,110,115] but the irreversibly bonded monolayers do not undergo an annealing process similar to that occurring in Au/thiol SAMs.

Examples of molecular junctions are given in Table 2.

3. Single-Molecule Molecular Junctions

One could argue that single-molecule junctions are the most elegant, not only because they represent the lower limit in dimensions for molecular electronics, but also because their behavior is not complicated by intermolecular interactions. Although the fabrication and characterization of single-molecule junctions present formidable technical problems, their electron-transfer behavior should be related to that of the well-studied donor−acceptor molecules. Combined with the ability to theoretically model single-molecule junctions, the D−B−A precedent provides a good initial base for understanding the structural factors which control single-molecule conductance in molecular junctions.

3.1. Scanning Probe Microscopy (SPM). SPM in the form of scanning tunneling microscopy (STM) and conducting probe atomic force microscopy (CP-AFM) were natural techniques for early experiments on single-molecule conductivity,[116] with the junction being formed by the substrate, monolayer, and SPM tip (Figure 7). The STM or CP-AFM tip interacts with one or a few molecules, and the "single" molecule involved in the junction need not be isolated from its neighbors (necessarily). In CP-AFM, the junction is similar, but the pressure of the top contact on the molecule is controlled, rather than the tunneling current.

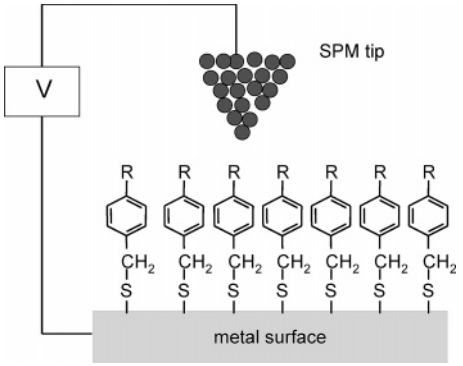

Figure 7. Schematic of a molecular junction composed of a monolayer on a metal surface and a top contact from a scanning probe microscope. The SPM tip may be a metal probe of a scanning tunneling microscope or a conducting tip of an atomic force microscope.

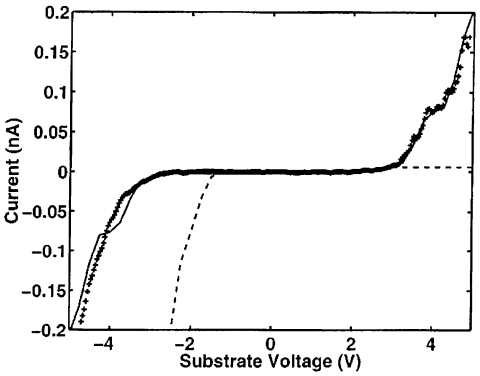

Figure 8. Current/voltage curve of xylyldithiol obtained with STM: +, experimental observations; solid and dashed lines, theoretical curves for η (defined in Figure 10) of 0.5 and 0.0, respectively. Adapted from ref 118.

Kubiak et al.[99,117−123] reported an early STM study of a xylyldithiol monolayer on gold which yielded the current/voltage curve shown in Figure 8. Distinct steps in the current response were considered strong indications that the conductivity is controlled by a molecular property, most likely the matching of the Fermi level of a metal contact to the HOMO of the molecule. In such a case, the HOMO provides a channel for ET through the junction, which should be much more efficient than tunneling. The importance of the molecule−tip distance was emphasized, and was included as an adjustable parameter during comparisons to theory. An alternative and often more useful representation of *i*/*V* curves for molecular junctions is shown in Figure 9, for the same xylyldithiol junction structure shown in Figure 8. The differential conductance, d*I*/d*V*, plotted vs *V* accentuates the current steps of Figure 8, but more importantly is related to fundamental concepts in STM. Equation 5

$$g_o(V) = \frac{dI}{dV} = \left(\frac{2e^2}{h}\right) T(E_f + eV) \qquad (5)$$

shows that d*I*/d*V* is a product of a transmission factor, *T*, and a factor incorporating the electron charge, *e*, and Planck's constant, *h*. If the transmission factor has its maximum value of 1.0, g_o equals the quantum mechanical limit[119,124,125] for single-molecule conductance, $2e^2/h$, or $(12.9\ \text{k}\Omega)^{-1}$.

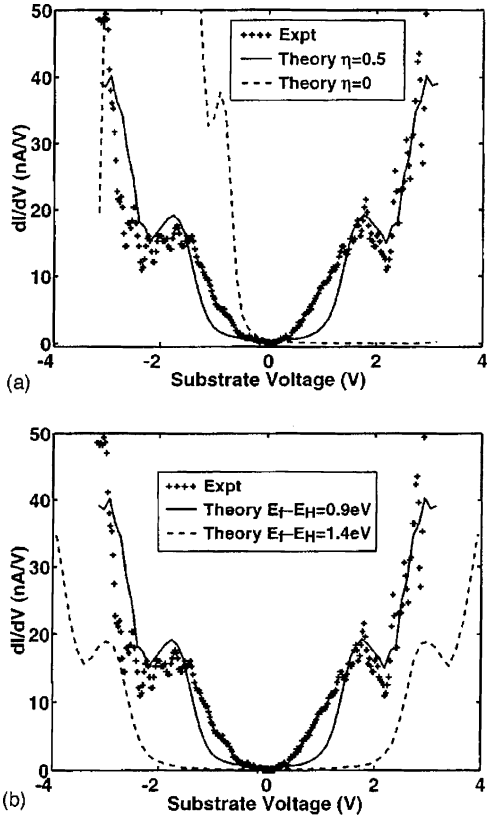

Figure 9. Differential conductance vs substrate voltage for a xylyldithiol monolayer probed with STM: +, experimental observations; solid and dashed lines, theoretical curves for the various conditions shown. Adapted from ref 123.

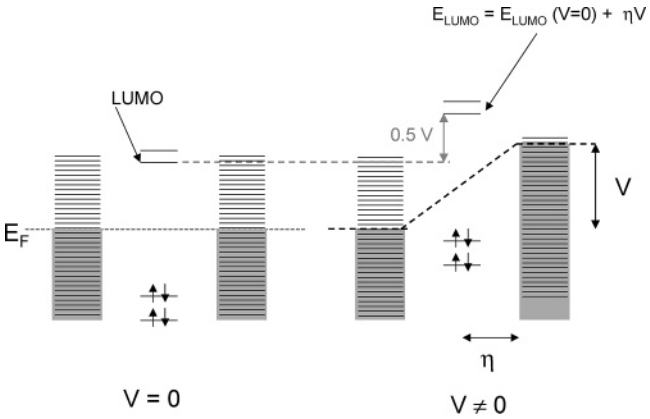

Figure 10. Energy level diagrams showing the effect of an applied voltage on the energy of the LUMO, for the case of a molecule positioned symmetrically between two contacts in a linear electric field. In the simple case shown, the molecular orbitals are all shifted together in response to the applied voltage. See refs 118−120 and 123 for a detailed explanation.

Kubiak et al. proposed a parameter to characterize how the electric field within the junction affects conductance.[118] The energy of the orbitals in the molecule depends on the local potential relative to the Fermi levels of the contacts. For example, an orbital positioned at the midpoint between the contacts in a linearly varying electric field has an energy displaced by $^1/_2V$ from the Fermi level of both contacts (Figure 10). Unfortunately, the potential profile is usually unknown and difficult to determine, so the HOMO energy (for example) is difficult to determine. As will become apparent below, the potential profile is very often a

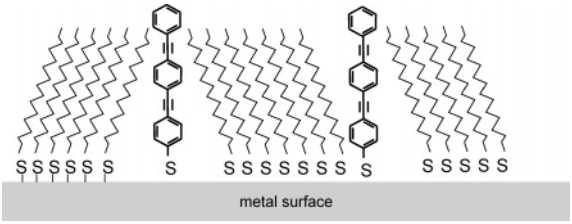

Figure 11. Schematic of a mixed monolayer of phenylethynyl thiolates diluted by alkanethiols, in which the conjugated molecules exhibit higher tunneling probability. See refs 98 and 126−128 for a detailed description.

"sticking point" in attempts to correlate theory and experiment.

The STM results shown in Figures 8−10 and their associated papers reinforce the point made earlier that conductivity in even a single molecule is not a simple issue, involving (at least) the Fermi levels of the contacts, the molecule/contact interface, and the electric field profile in the junction. These variables are in addition to the energy levels associated with the molecule and how they are influenced by a possibly large applied electric field. It has not been easy to determine which of these or other factors control conductivity. In addition, the temptation to cite a "single-molecule resistance" should be tempered by an appreciation that molecules may exhibit complex, nonohmic behavior. A single-molecule resistance may provide an indication of relative conductivity at low bias, but it is already clear that molecules do not behave like classical resistors except under highly restricted conditions.

Weiss et al. studied a longer molecule by STM in a study contemporary with that of Kubiak et al.[98,116,126−129] Phenylethynyl oligomers have been proposed as "molecular wires" due in part to their rigid, linear, highly conjugated structures. A mixed monolayer of the phenylethynyl molecule shown in Figure 11 was prepared, with the majority of the monolayer being an alkanethiol. An enhanced STM current was observed at randomly distributed points in an STM image of the mixed monolayer. These points of high current were attributed to higher conductivity through the conjugated phenylethynyl molecule, relative to the surrounding alkanes. In a related paper, some nontrivial effects of the tip−molecule spacing, and how they affect the STM image, are discussed.[98,128] The mixed monolayer depicted in Figure 11 also exhibited an unexpected effect attributed to conductance switching. Randomly oriented sampling positions on the mixed monolayer exhibited stochastic "switching" between high-conductivity and low-conductivity states, as evidenced by random variation in the observed STM height.[126] These spots appeared to switch on and off randomly with time and repeated STM scans, and the effect was proposed to originate in conformational changes in the phenylethynyl molecule. The effect of substituents was examined, but a detailed structural basis for conductance switching was not revealed. Gorman et al. reported that stochastic switching occurred in redox-active thiol monolayers with different structures, and also proposed a conformational mechanism.[130] In a subsequent report from a third laboratory, it was noted that similar conductance changes were observed for alkanethiols, and more rapid switching at higher temperature.[131] Since a molecular mechanism for conductance changes in alkanes is hard to imagine, it was proposed that the conductance switching was actually due to repeated breaking and re-forming of the Au−S surface bond.

Bard et al.[132,133] used STM combined with sheer force microscopy to determine *i/V* curves for a variety of conjugated and nitro-substituted SAMs on Au. A threshold voltage for the onset of a dramatic current increase was observed to depend on molecular structure, and β values were determined as a function of voltage. Several of the monolayer structures studied exhibited one or more spikes in the *i/V* curve, attributed to negative differential resistance (NDR), which was first reported for larger molecular junctions (section 4.2). They also reported that molecules with nitro groups can store electrons in the monolayer, presumably by formation of an anion radical. Preliminary results comparing a Au−aryl surface bond to a Au−S−aryl bond showed a significant reduction in threshold voltage in the absence of the sulfur atom, implying a larger electron injection barrier for the Au−S bond. In a subsequent paper the NDR peaks were correlated with the reduction potentials of the SAM molecules and the energy of the LUMO of each molecule.[133] There was a 1:1 correspondence between the number of negative NDR peaks and the number of low-lying LUMOs of the molecules studied. Furthermore, the correlation of reduction potentials, LUMOs, and NDR peaks strongly suggests that an electron may be injected into the molecule's LUMO when the applied voltage corresponds to a LUMO energy,[134] resulting in a current spike. A similar correlation of redox properties and tunneling was reported earlier by Hipps et al., for tunneling junctions consisting of metal phthalocyanines and porphyrins doped into aluminum oxide between aluminum and Pb contacts.[135−138] Resonant tunneling through LUMOs which might also be involved in a redox process was observed, with both inelastic tunneling spectroscopy and STM.[135] A more recent study of monolayers of heteropolyacid catalysts (e.g., $H_3PMo_3W_9O_{40}$) on graphite also demonstrated a correlation of NDR behavior observed in STM experiments with electrochemical reduction potentials in solution.[139] Furthermore, Gorman et al. showed that the peak NDR voltage of ferrocene-containing SAMs probed with STM could be shifted systematically by varying the composition of the junction.[140] Although there is not yet a consensus on the mechanism of NDR observed with STM experiments, the correlation of LUMO energies, reduction potentials, and NDR peak voltages provides strong evidence for a mechanism involving resonant tunneling through the molecule's LUMO.[124,133,135,139,140]

A recent report of rectifying molecular junctions by Ashwell et al.[141] is based on STM junctions of the type Au(substrate)−S−$C_{10}H_{21}$/D−π∠A−$C_{10}H_{20}$−S−Au(tip), where D−π−A represents a donor−acceptor molecule with a conjugated bridge. Rectification ratios of 5−18 (at 1 V) were observed, depending on the lengths of the alkane chains. A change in the orientation of the D−π−A moiety caused reversal of the rectification direction, as did exposure to HCl vapor, which protonated a quinoline-containing D−π−A segment. The change in rectification direction with structural changes in the molecular layer supports a molecular mechanism for rectification, rather than some property of the

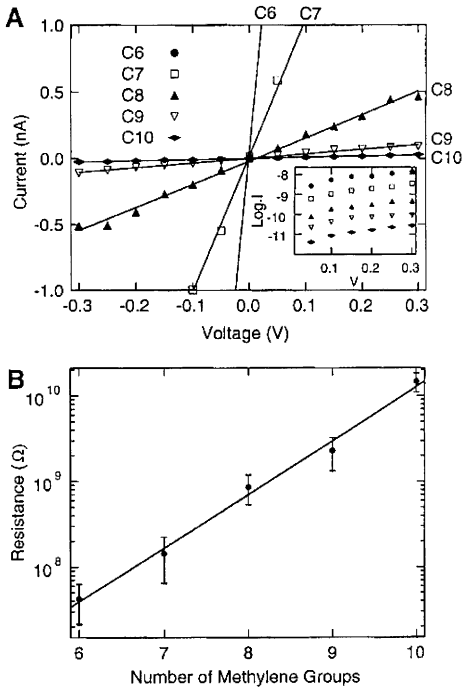

Figure 12. Current/voltage curves at low bias for CP-AFM experiments of a series of alkanethiol monolayers, all acquired with a tip force of 2 nN. The lower plot shows the dependence of the resistance on the chain length, resulting in a β of 1.45 per CH_2 unit. Adapted from ref 143.

Table 3. Observed d*V*/d*i* for Single Molecules, Ω

tip/molecule/substrate	method	d*V*/d*i*	note	ref
Au/xylyldithiol/Au	STM	$(18 \pm 12) \times 10^6$	a	117
Au/decane thiol/Au	CP/AFM	$>1.3 \times 10^{10}$	b	59
Au/dodecanedithiol/Au	CP-AFM	$(8.3 \pm 1) \times 10^9$	b	147, 149
Au/phenyldithiol/Au	BJ[c]	2.2×10^7	a	155
Au/bipyridine/Au	BJ	1.3×10^6		125
Au/decanedithiol/Au	BJ	6.3×10^8		125
Au/benzenedithiol/Au	BJ	1.2×10^6		158
Au/xylyldithiol/Au	BJ	2.1×10^7		158
Au/dodecanedithiol/Pd	nanowire	2×10^{11}	d	184

[a] Reported for the first plateau of the d*i*/d*V* vs *V* curve. [b] Low-voltage resistance. [c] BJ = break junction. [d] Per molecule, from a 3500-molecule junction.

contacts. Several examples of molecular rectifiers which do not involve STM are discussed in section 5.1.

CP-AFM has been used to make and study thiol monolayers on Au.[59,131,142−147] The force exerted on the molecular layer was variable, and 2 nN was found by Frisbee et al. to yield reproducible *i*/*V* curves.[143] Higher force resulted in larger currents until penetration of the SAM occurred at ~100 nN. The current/voltage response was linear for small bias (±0.3 V), and a semilog plot of the observed junction resistance vs the number of CH_2 units in the alkanethiol was linear with a slope of 1.45 per methylene unit (Figure 12). The junction resistance for decanethiol and 2 nN force was 1.3×10^{10} Ω, which is listed with other reported values for single-molecule resistance in Table 3. The CP-AFM approach yielded good reproducibility and a clear exponential dependence on molecule length. However, the number of molecules involved in conduction is uncertain, but apparently quite consistent. The resistance listed in Table 3 is $>1.3 \times 10^{10}$ Ω for a single decanethiol molecule, since multiple parallel conductance paths should reduce the observed resistance.

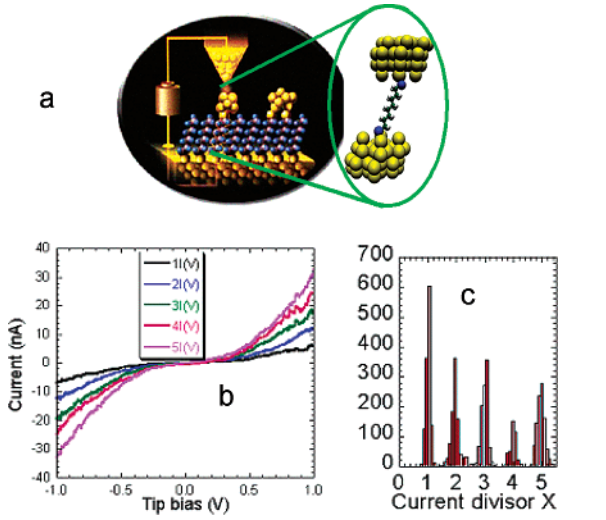

Figure 13. (a) Schematic of an octanedithiol monolayer with a Au nanoparticle top contact, probed with CP-AFM. (b) Series of *i*/*V* curves observed for several nanoparticles, showing quantization of the observed current. (c) Histogram of the observed current multiplier for a large number of junctions. The observed current was approximately an integer multiple of a "fundamental curve", the smallest observed in panel b. See refs 131, 142, and 147−149 for details.

Both Kubiak et al. and Lindsay et al. have used gold clusters to reduce the uncertainty associated with the tip/molecule interface.[117,121,122,131,146,148] A dithiol molecule adsorbed conventionally on a Au surface has pendent SH groups which can react with Au nanoparticles. The particle/molecule/substrate assembly is a nearly symmetric molecular junction which may be interrogated with an STM or CP-AFM probe. A schematic diagram and representative results are shown in Figure 13. The particle/molecule/substrate structure with covalent Au−S bonds at both ends yielded two important conclusions. First, the conductance was much higher when a covalent bond existed at both ends of the molecule, indicating faster ET for the covalent contact over the physisorbed contact. Second, a series of *i*/*V* curves was observed for different probe positions, as shown in Figure 13b. At all points along these curves, the current was an integral multiple of a "fundamental curve" with the smallest current.[148,149] A histogram of these integer multipliers for >1000 junctions is shown in Figure 13c. The authors argue that the apparent quantization of conductivity could be caused by the CP-AFM tip contacting multiple particles or by a given particle being bonded to multiple molecules in parallel. In either case, the "fundamental" *i*/*V* curve must be that of a single molecule suspended between the Au substrate and the Au nanoparticle, with covalent Au−S bonds at both ends.

Finally, a few examples are available of spectroscopic probes of electron transfer in single-molecule or monolayer devices, based on STM,[150] single-molecule fluorescence,[151] inelastic tunneling spectroscopy (IETS), and Raman spectroscopy.[135,138,152−154] Scanning tunneling spectroscopy of Au/Cu(phthalocyanine)/Au junctions revealed the distribution of electrons over the bridge molecule, and the density of electronic states on an isolated bridge molecule as well as a molecule coupled to a varying number of Au atoms.[150] IETS provides vibrational information about a bridge molecule, by the

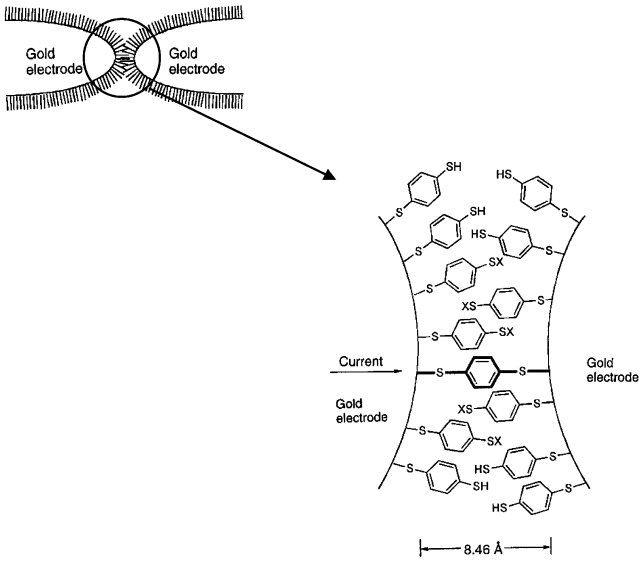

Figure 14. Break junction consisting of a break in a Au wire spanned by one or more phenyl-1,4-dithiol molecules. Adapted from ref 155.

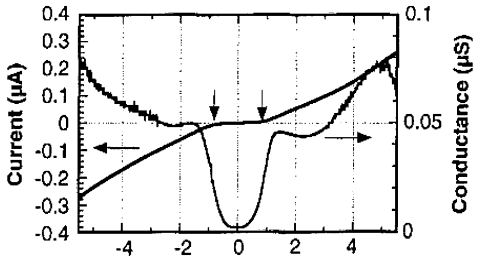

Figure 15. Current (left axis) and differential conductance (right axis) for a phenyldithiol break junction. Adapted from ref 155.

effect of the molecule's structure on a tunneling electron.[135,153,154] Although STS and IETS generally require liquid helium temperatures, they provide direct probes of structure in junction molecules. Given the difficulty in characterizing single-molecule or monolayer devices in operation, it is likely that spectroscopic probes of molecular junctions will become more important with time.

3.2. Break Junctions. A break junction provides a means to suspend one or a few molecules between conducting contacts formed by breaking a thin metallic conductor to form a very narrow gap. An early example reported by Reed and Tour in 1997[155−157] stimulated both excitement and controversy, as well as extensive theoretical modeling. As shown schematically in Figure 14, the gap between two Au contacts was controlled by piezoelectrically stressing a "bending beam" substrate on which a gold wire was vapor deposited. A break in the gold occurred when the beam was stressed, and the gap width was a monotonic function of the stress applied. After the gap was formed, a solution of phenyldithiol was introduced, and one or more dithiol molecules bridged the gap to form a molecular junction. The observed current and differential conductance are shown in Figure 15. The conductance corresponding to the first step in the dI/dV curve corresponded to a resistance of 22 MΩ, close to that reported for the xylyldithiol junction probed with STM.[117]

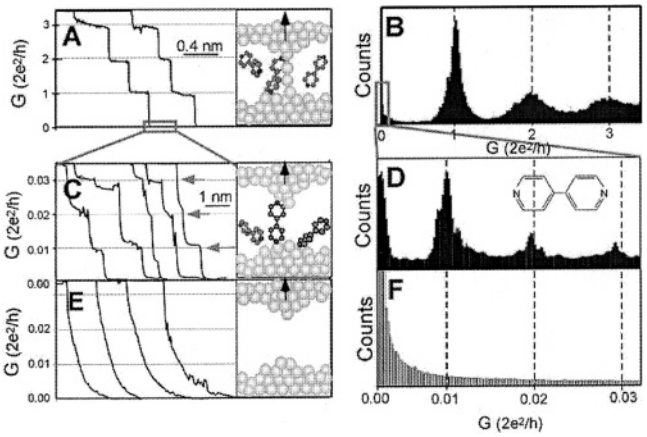

Figure 16. (A), (C), and (E) are conductance vs time curves as a Au STM tip is drawn away from a Au surface after contact in a solution of 4,4′-bipyridine. (B), (D), and (F) are histograms of 1000 measurements, plotted as the observed conductance in units of $2e^2/h$. Reprinted with permission from ref 125. Copyright 2003 American Association for the Advancement of Science.

A conceptually similar approach by Xu and Tao had the same objectives as the Reed and Tour experiment but had the advantage of permitting a large number of break junctions to be observed and analyzed statistically.[125,158] A gold STM tip was repeatedly contacted with a Au surface in a solution of a dithiol or bipyridine. As the probe was lifted slowly off the surface, gold atoms formed a nanofilament and then a break junction. A 4,4-bipyridine molecule in solution (for example) presumably bridged the gap as the break formed, and the conductance was monitored throughout withdrawal of the probe. The results show discrete steps of conductance corresponding to formation of a Au filament, then a bipyridine molecular junction, and then an open gap (Figure 16A,C,E). A histogram of 1000 such experiments (Figure 16B,D,F) shows that the observed conductance falls into a pattern of discrete values, with the Au nanofilament exhibiting the maximum value of $2e^2/h$. On the basis of these results, the low-voltage resistance of a single 4,4′-bipyridine molecule is 1.3 ± 0.1 MΩ, which is listed along with several other resistance values in Table 3. For the case of decanedithiol, the observed resistance was 630 MΩ, and a determination of β from three alkanedithiols yielded a value of 1.04 ± 0.05 per CH_2 unit. In addition, β was found to be weakly dependent on the bias in a fashion consistent with a 5 eV energy gap between the HOMO of the molecule and the Fermi level of the contacts. The theoretical model assumed a linear potential profile in the junction, with the HOMO assumed to reside at the midpoint of the profile.

4. Monolayer Molecular Junctions

As noted in the Introduction and Scope, monolayer molecular junctions are related historically to both organic thin film devices and redox polymer films between two conductors. We are restricting the discussion here to junctions involving a molecular monolayer with at most a few subunits and a thickness of less than 50 Å. Redox concepts are often invoked in discussions of molecular junctions, since they involve electron transfer, reorganization energy, and electric fields. Our

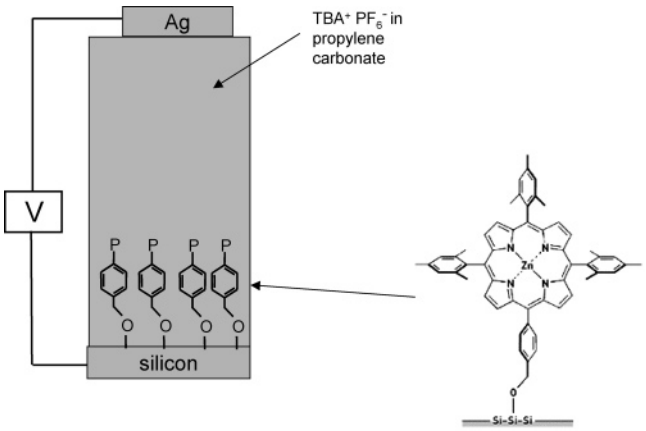

Figure 17. Redox storage cell currently under development by ZettaCore, Inc. The porphyrin redox center (P) is oxidized to a cation to effect charge storage in a memory device. Read/write cycles have been repeated 10^{12} times with minimal degradation. The structure (right) is reprinted with permission from ref 106. Copyright 2003 American Association for the Advancement of Science. See also refs 160, 163, 165, 168, and 169.

discussion will start with a redox-based molecular junction in which the concepts are well understood and then progress to thinner junctions in which electron transport through the junction is more direct, but the mechanism less clearly understood. Note that the redox junction discussed in section 4.1 is not the first example of a monolayer molecular junction, but serves as a conceptually useful starting point.

4.1. Redox Charge Storage Junction. A monolayer molecular junction introduced in 2000[159,160] is currently under development as a commercially viable alternative for computer random access memory.[161−164] The structure shown schematically in Figure 17 is an electrochemical cell with a monolayer of porphyrin redox centers acting as one of the half-reactions. As is well-known for electrochemical cells, charge transport between the conducting contacts involves electrons at the two contact surfaces, ions in the electrolyte, and faradic reactions to convert between electron flow and ion flow. In the case of the structure of Figure 17, the positive charge stored by the oxidized porphyrin persists for several minutes at open circuit, so the charge state of the porphyrin layer is the basis of a memory device.[101,102,159,160,165−171] The porphyrin monolayer was shown to be tolerant of processing in a production environment at 400 °C, and the 0/+1 redox reaction could be cycled at least 10^{12} times.[106] These attributes make a porphyrin-based redox junction attractive for incorporation into silicon microelectronic devices, and a prototype 1 MB molecular memory chip is currently being tested.[163]

Although the active region of the redox junction is a monolayer, the electron transport and charge storage of interest to possible electronic applications are accompanied by ion motion and redox reactions. Snyder and White (1995) investigated redox "junctions" in which the electrolyte layer was made very thin, to model how an STM tip interacts with a redox-active monolayer.[172] As a layer of solution containing $Fe(CN)_6^{4-}$/$Fe(CN)_6^{3-}$ was made progressively thinner, the observed current exhibited the symmetric, sigmoidal response of Figure 18. This behavior was compared to that of a

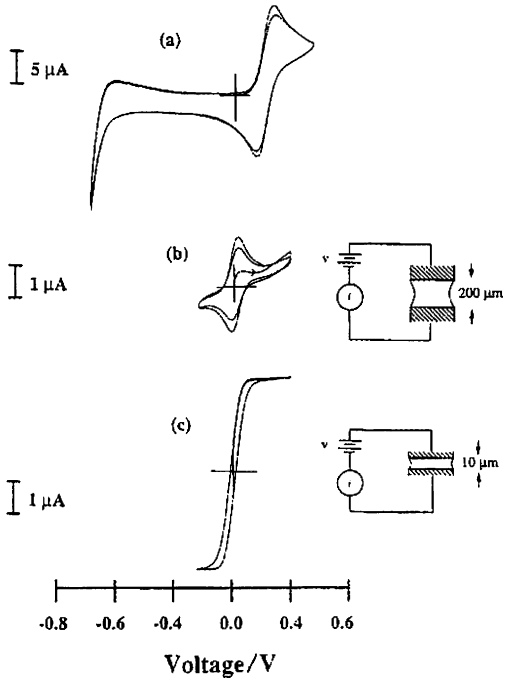

Figure 18. Voltammetry of a ferri/ferrocyanide redox couple in bulk solution (a), a 200 μm thin layer cell (b), and a 10 μm thin layer cell (c). As the cell becomes thinner, the mass transport rate increases, and the response approaches a sigmoid. Reprinted from ref 172. Copyright 1995 Elsevier.

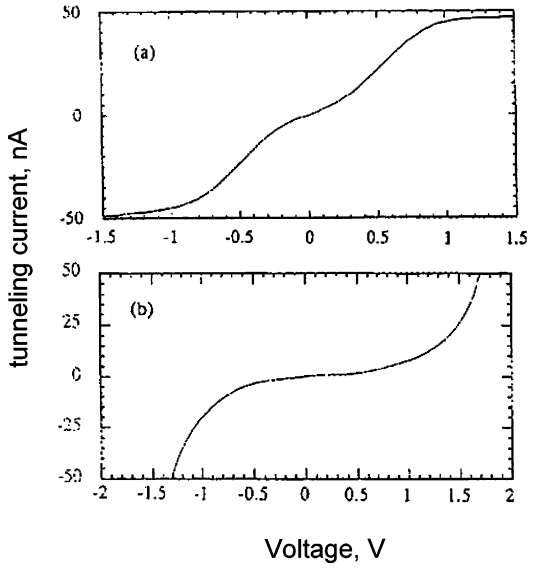

Figure 19. Current/voltage curves of graphite/porphyrin/STM junctions, for an iron porphyrin near monolayer (curve a) and thin film (curve b). Reprinted with permission from ref 172. Copyright 1995 Elsevier.

porphyrin monolayer on graphite, in which a layer of the redox-active molecules lies flat between a conducting substrate and the STM tip. For a multilayer of iron(III) porphyrin, the *i*/*V* curve of Figure 19b was observed, whereas a near monolayer yielded Figure 19a. The STM *i*/*V* curves were obtained in the absence of solvent or intentional counterions. The observed currents in the STM experiments were attributed to electron transport by one or more redox events, in which an electron injected from the negative tip reduces Fe(III) to Fe(II) and then the Fe(II) transfers the electron either to the positive substrate or to another Fe(III)

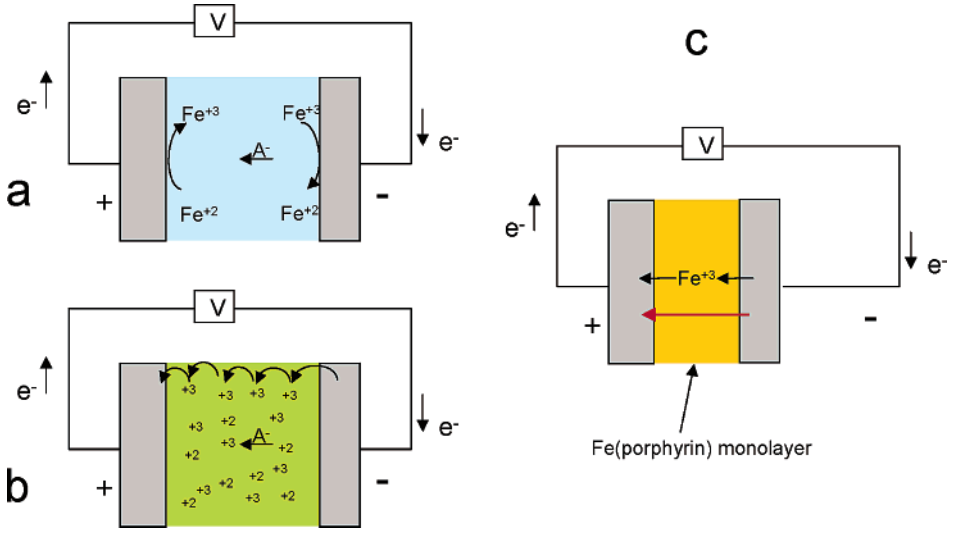

Figure 20. Schematic electron transfer in a conventional electrochemical cell (a), a redox polymer thin film (b), and a monolayer tunneling junction (c). Charge is carried by mobile ions in the electrochemical cell, following conversion of electrons to ions by a faradic reaction.[172] In a redox polymer, electrons may hop from center to center, with or without motion of a counterion.[22] In the tunneling junction, the electron may tunnel directly (red arrow), or resonantly through the LUMO of the redox center.[133] The figure uses iron(II/III) porphyrin as an example, with A^- representing a generic anion.

center. This experiment is distinguished from the redox monolayer cell of the previous section and from redox polymer thin films[22] with regard to the role of counterions. As the molecular layer thickness approaches a monolayer, there must be a point where counterions are absent or irrelevant. The electron transfers directly from the negative contact into the redox center (presumably into its LUMO) and then into the positive contact. In contrast to a conventional redox cell, electron transport need not be accompanied by ion transport. Although the model of a thin layer redox cell is macroscopic, it embodies the same concepts as the STM experiments described in section 3.1 and Figure 19. Three electron-transfer mechanisms for metal/molecule/metal junctions are shown in Figure 20. These illustrations should be considered schematic, but they do indicate the progression from a redox cell to a tunnel junction with decreasing junction thickness. The common thread that is emerging from experiments in different laboratories is the relationship among reduction potential, LUMO energy, and rapid electron transfer in a tunnel junction.[133,135,139,172,173]

4.2. SAM-Based Monolayer Junctions. Some formidable technical issues arise in the investigation of monolayer junctions which involve many molecules in parallel. In the absence of electrolyte, the two conductors are separated by only a monolayer of organic molecules. Pinholes in the monolayer may permit metallic short circuits to occur, with presumably much higher conductivity than that of the molecules. Vapor deposition of a variety of metals on SAMs has been investigated in some detail, and the success of this method for making a top contact depends in part on reactions between the SAM and the metal. Allara et al. showed that Au and Ag atoms penetrate aliphatic SAMs, with the SAM reforming on top of the deposited metal.[96,97,128,174−176] It was possible to keep the metal on top of the SAM if it reacted with the SAM headgroup, e.g., Al on carboxylate-terminated SAMs. Ti caused destruction of aliphatic SAMs, as judged by mass spectrometry[176,177] and FT-IR.[178] FTIR of a naphthalene−alkane SAM showed that Ti disordered the aliphatic segment but left the naphthalene centers intact.[179] Due to concerns about defects in SAMs, many of the monolayer junctions studied to date have small areas, often as small as the domain size of the SAM.[86,180] Early examples of metal/SAM/metal junctions were conceptual extensions of STM and break junction experiments, motivated partly by the desire to examine molecular junctions which might be amenable to mass production in microelectronic devices.

4.2.1. Nanopore Junctions. The Reed and Tour collaboration investigated Au/monolayer/Au junctions incorporating the phenylethynyl molecule shown in Figure 21.[86,157,180−183] The junction was a circle of 30−50 nm diameter made with electron beam lithography and reactive ion etching. The authors estimated that each junction contained ~1000 oriented molecules, and reproducibility was sufficient to collect statistically significant results. Figure 21 shows an *i*/*V* curve for the "nanopore" junction at 60 K. The sharp peak at ~2.0 V is a clear signature of "negative differential resistance" (NDR). Unlike a conventional diode, whose differential resistance decreases but remains positive as the voltage is scanned, d*V*/d*i* for NDR becomes negative, in this case for $V > 2$ V. This phenomenon is quite unusual, and was an early stimulus to consider practical applications of molecular electronic devices.

In subsequent papers the temperature dependence for nanopore structures based on the asymmetric Au/thiobiphenyl/Ti junction[86] and a symmetric Au/1,4-phenylene diisocyanide/Au junction[181] is reported. As noted in Table 1, variations of current with temperature can be useful for distinguishing ET mechanisms. The asymmetric junction showed rectification, with larger currents when the Ti was negatively biased. The symmetric junction exhibited nearly symmetric *i*/*V* curves with minimal rectification. Both junctions showed a dependence on T and V consistent with thermionic emission across one of the metal/molecule interfaces, with a barrier height of 0.22 eV for the Ti/biphenyl interface and 0.35 eV for the Au/isocyanide interface. The authors concluded also that the Ti/phenyl "contact"

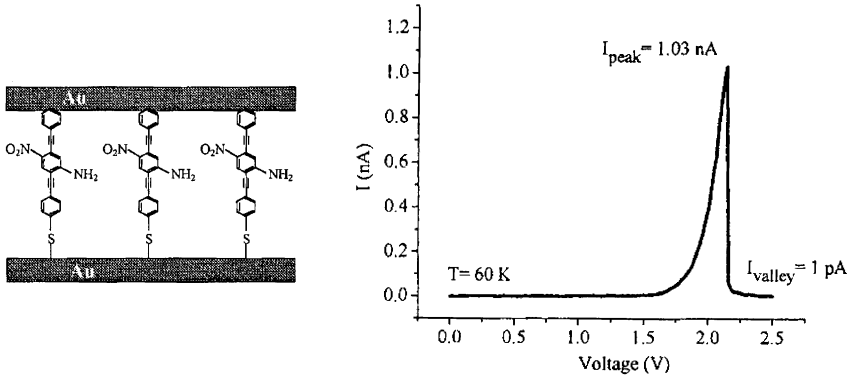

Figure 21. Structure (left) and *i/V* curve (right) of a nanopore junction made from phenylethynyl molecules substituted with amino and nitro groups. The peak current density is ~50 A/cm^2 on a junction of approximately 10^{-10} cm^2 area. Adapted from ref 156.

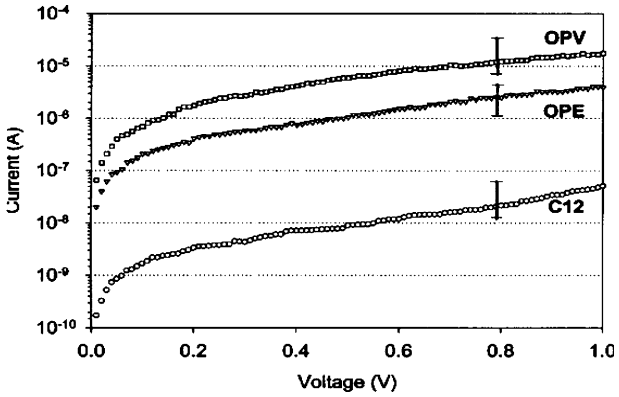

Figure 22. Semilogarithmic plots of current vs voltage for Au/SAM/Pd nanowire junctions formed from dodecanethiol (C12) and oligomers of phenylenevinylene (OPV) and phenyleneethynylene (OPE). Error bars are based on 10 or more nanowire junctions. Adapted from ref 184.

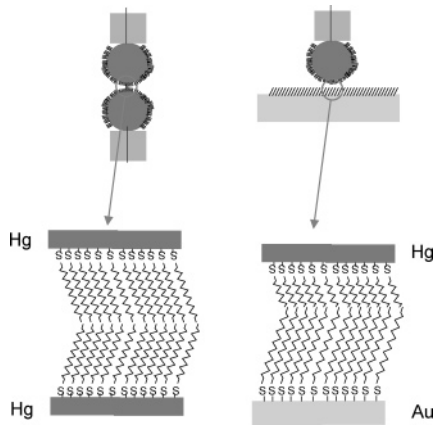

Figure 23. Schematic drawing of Hg/SAM/Hg and Hg/SAM/Au junctions. In both cases, the Hg drops are macroscopic (~1 mm diameter), and the drawings are not to scale. For the Hg/SAM/Hg junction, the two Hg drops are brought together in a solution of an alkanethiol. For the flat Au substrate on the right, the Hg drop is lowered through the thiol solution onto the preformed SAM on Au. See refs 60, 61, and 186−188 for details and results.

presented a lower energy barrier than the Au/S/phenyl contact.

4.2.2. Nanowire Junctions. A quite different junction design with a similar cross-sectional area was produced by Cai et al., using electrodeposition in ~100 Å diameter pores in polycarbonate membranes.[184] A first metallic contact was electrodeposited in a large collection of pores, and then a dithiol was allowed to adsorb to the contact surface. After a second metal contact was deposited, the polycarbonate was dissolved in methylene chloride to yield a large number of nanowire junctions. Individual wires were suspended between metal electrodes spaced 3−5 μm apart for electronic characterization. The *i/V* curves were generally symmetric, with a strong dependence of current on molecular structure. Semilogarithmic plots of current vs voltage for single nanowires are shown in Figure 22 for three dithiol molecules. The larger resistance compared to that of the CP-AFM experiment on the dodecanedithiol molecule (Table 3) was attributed to differences in contacts and sample preparation.

The conductance of nanowire junctions made from conjugated dithiols was significantly higher than for the alkanedithiols, by 2−3 orders of magnitude for conjugated oligomers with lengths similar to that of dodecane (Figure 22). The phenylethynyldithiol showed both larger currents and a lower voltage threshold for increased conductivity. The authors reported a smaller voltage gap between the positive and negative onsets of increased conductivity, in the order 0.2 V for phenylvinyl (OPV), 0.7 V for phenylethynyl (OPE), and 1.2 V for dodecane (C12).[184] This sequence was attributed to the smaller energy gaps for the conjugated molecules, and is consistent with the order observed for ET through similar monolayers in electrochemical investigations in solution. In addition, the conductivity for Pd contacts was higher than that observed for Au contacts, a difference which was attributed to better metal−molecule electronic coupling for Pd than for Au.

4.2.3. Mercury/SAM Molecular Junctions. The laboratories of Majda et al.[185−187] and Whitesides et al.[61,188] reported molecular junctions made between two mercury drops or between Hg and a solid metal (Ag, Au, Cu). One motive for this junction design was ease of fabrication, which permitted observation of a statistically significant number of junctions, and avoided lithography and the risk of monolayer damage by vapor-deposited top contacts. Furthermore, the high surface tension of Hg should reduce the likelihood of metal penetration into the SAM, thereby reducing the likelihood of short circuits. Two junction designs are shown in Figure 23; in both cases the junction was formed while the Hg drop(s) was immersed in a solution containing the SAM of interest. It is important to note

that the Hg/SAM interface is much larger in area than the "nanopore" and "nanowire" junctions, measuring 01−1.0 mm in diameter and containing 10^{11}−10^{13} molecules.

The original papers should be consulted for the detailed experimental and theoretical investigations of Hg/SAM junctions, but several conclusions deserve special note. First, the junction conductance depended strongly on the junction thickness, with observed β values of 0.8−1.0 Å^{-1} for well-ordered alkanethiols. For phenylene oligomers, β decreased to 0.61 Å^{-1}. Second, the junction capacitance varied with thickness, in a manner quantitatively consistent with that of a parallel plate capacitor having a dielectric constant close to 2.0.[186,187] This value is expected for hydrocarbons, so the junction capacitance provides good support for the structural model shown in Figure 23. Third, the bilayer Hg/SAM/metal junctions exhibited very large current steps at high voltage (2−4 V), attributed to dielectric breakdown. The electric field at breakdown was 10^6−10^7 V/cm, which is consistent with breakdown fields of bulk materials.[189] Fourth, the Simmons tunneling model with a rectangular barrier was *not* adequate for quantitatively describing junction behavior. The observed β for Hg/SAM/Hg junctions did not depend strongly on the applied voltage,[187] and the observed currents were significantly larger than predicted from the Simmons model. A parabolic barrier yielded predictions closer to the experimental currents,[61] but necessarily involved an additional adjustable parameter. Finally, the existence of opposing SAMs on the two contact surfaces permitted asymmetric Hg/SAM$_1$/SAM$_2$/metal and related junctions to be studied with a variety of molecular structures.[61,185,188] Such junctions exhibited asymmetric *i*/*V* curves which were modeled theoretically.

A related paradigm involving a Hg drop is described in section 6.2.1 rather than here, because it does not involve a thiol-based SAM.[190−192] In the laboratory, the Hg-based junctions provide a convenient test bed while the molecular structure and substrate are varied, but they are mechanically unstable and not amenable to incorporation in a practical microelectronic device. In my opinion, they are indeed useful test beds, but practical devices will require alternative, more rugged junction structures which are amenable to massively parallel fabrication.

5. LB Molecular Junctions

The LB technique for constructing monolayers or multilayer films is well characterized and is not restricted to thiols or Au surfaces. A molecule with a hydrophilic "head" and a hydrophobic "tail" will orient on the surface of water. The resulting film is compressed laterally until monolayer formation is detected by a change in surface tension. This monolayer may be transferred to metal or metal oxide surfaces, with its order and density maintained. The LB approach provides good control of coverage and leads to a well-defined structure, but the bonding to the substrate is usually electrostatic and weak compared to the Au−thiol bond. Hence, the junction is prone to disordering upon metal deposition or with time after fabrication.

5.1. LB Molecular Rectifiers. Metzger et al. have used LB techniques to construct and investigate molecular rectifiers based on donor−acceptor molecules.[87,88,91,193−199] The Au/molecule/Au junctions are experimental manifestations of the original Aviram and Ratner proposal of 1974.[37] The energy level diagram of a DBA molecule in a molecular junction is shown in Figure 24. The acceptor molecule has a relatively low energy LUMO, while the donor has a relatively high energy HOMO. For the voltage depicted in Figure 24, an electron may transfer into the acceptor LUMO, accompanied by ET out of the donor HOMO, resulting in a $D^{+-}B-A^-$ excited state. The electron transfers are fast if the orbitals align with the metal Fermi levels as shown. Intramolecular ET from A^- to D^+ completes the transfer of one electron from the right contact to the left. Note that the reverse ET is energetically uphill; hence, rectification results, with fast ET from right to left in Figure 24.[91]

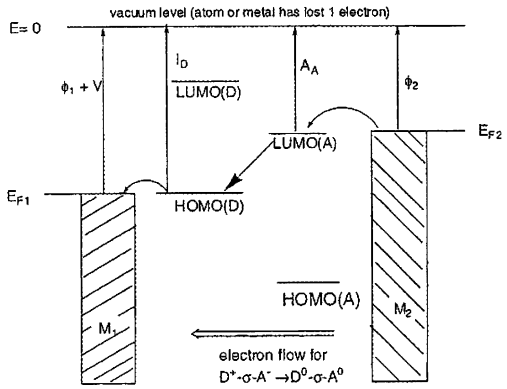

Figure 24. Aviram−Ratner model for a molecular rectifier based on a donor−acceptor molecule. Φ_1 and Φ_2 are the work functions of the two metal contacts, and V is the applied voltage. As drawn, facile electron transfer is from the Fermi level of metal 2 (M_2) to the LUMO of the acceptor, and from the donor HOMO to metal 1 (M_1). Reprinted from ref 91. Copyright 2003 American Chemical Society.

The Metzger group studied a variety of D−B−A molecules which exhibited rectification, for both symmetric junctions with contacts of the same metal and asymmetric junctions with different metals. The case of hexaqdecylquinolinium tricyanoquinodimethide is shown in Figure 25. This junction had Au for both contacts, with the top contact deposited slowly while the sample was cooled with LN_2. The polarity of the *i*/*V* curve in Figure 25 corresponds to rapid ET from the acceptor to donor, as predicted from Figure 24. The Au junctions showed current densities 3−5 orders of magnitude higher than those for aluminum oxide contacts, due to decreased contact resistance.[87] The current density for an applied voltage of 2 V was 0.3 A/cm^2 or $\sim 10^4$ (e$^-$/s)/molecule. However, the rectification degraded with repeated scanning, with the rectification ratio ($J_+/-J_-$) at 2 V decreasing from 27.5 to 1.9 during five voltage scans. Degradation was attributed to disordering in the alkane chains due to transport of hot electrons, or to chemical degradation of the A^- excited state.

A related but distinct molecular rectifier structure used an asymmetric molecule, 2-tetradecoxynaphth-6-ylpropanethiol.[179] The molecule has an aliphatic chain and an aromatic naphthalene center. Although the molecule was bonded to Pt by a Pt−S linkage, it is appropriate to compare it to the LB rectifiers just discussed. The top contact was titanium, applied by

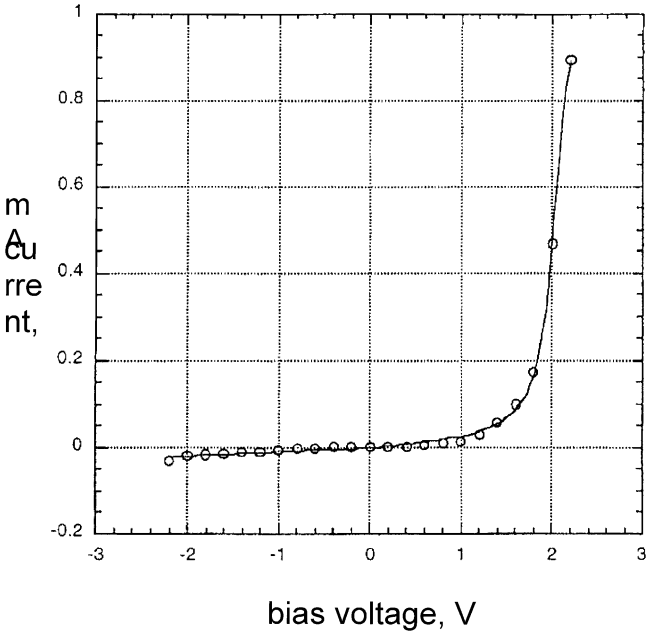

Figure 25. Current/voltage curve for an LB monolayer of hexadecylquinolinium tricyanoquinodimethide with gold contacts on the top and bottom. The direction of electron flow at positive bias is from the cyanoquinodimethane end to the quinolinium end of the junction molecule. Reprinted from ref 87. Copyright 2001 American Chemical Society.

electron beam deposition. FTIR showed that the Ti disordered the alkane portion of the monolayer, but had little effect on the aromatic center. A high current density (160 A/cm^2 at 2.3 V) and a high rectification ratio ($>5 \times 10^5$ at 2.3 V) were reported, and attributed to the action of naphthalene as a quantum dot. Although these values are higher than those shown in Figure 25 for an LB rectifier, the fact that the contacts are made from different metals complicates interpretation of the rectification mechanism.

5.2. Conductance Switching in LB Junctions. The significant economic value of molecular electronic switches stems from their possible utility as logic and memory devices. Whether one molecule or many in parallel are used as switches, the result would be a potentially much higher density of active devices than is currently possible with silicon or CMOS electronics. The basic concept of conductance switching is a reversible change in conductance caused by some electrical stimulus. However long the conductance remains in a low or high resistance state, it can act as a memory or logic element. As with existing memory devices, the performance of a molecular memory cell is judged by speed, persistence, power consumption, and device density. If the conductance of a molecule can indeed be repeatedly switched between persistent "on" and "off" states, it could be the basis of nonvolatile, high-density, low-power molecular memory.

An early approach to memory devices using LB structures was based on interlocking organic molecules rotaxanes and catenanes developed at UCLA.[46,89,92,200−204] Figure 26 shows a "rotaxane" structure, consisting of a viologen-containing "ring" around a "post" containing a tetrathiafulvalene (TTF) center. Note that the post has hydrophobic and hydrophilic ends to permit assembly of an oriented monolayer with the LB technique. The

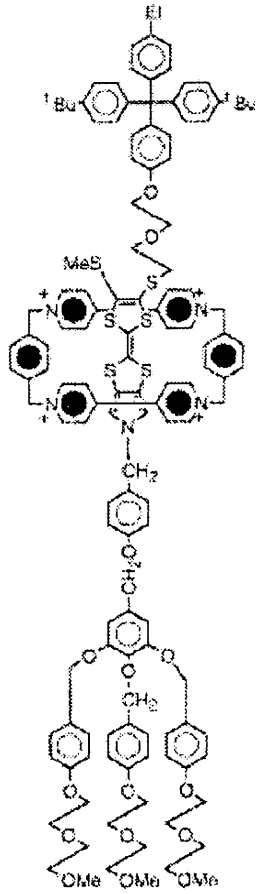

Figure 26. Structure of the a "single-station" rotaxane molecule, with a hydrophilic base, hydrophobic tail, and viologen-containing ring. Reprinted from ref 201. Copyright 2001 American Chemical Society.

rotaxane monolayer was positioned between a thin layer of Al_2O_3 on Al or silicon (hydrophilic end) and a vapor-deposited Ti/Al top contact (hydrophobic end). A current/voltage curve shown is in Figure 27, with the polarity defined as the Al/Al_2O_3 contact relative to the Al/Ti contact. The devices exhibited a sudden decrease in resistance at about −2 V, which could be reversed at positive voltage.[92,204,205] The high- and low-conductivity states implied a bistable "switch," and these states could be accessed repeatedly during potential cycling. The observations were interpreted with a mechanism based on motion of the viologen ring along the TTF post, accompanied by oxidation or reduction of the rotaxane supermolecular structure. Although the switching rate was slow by microelectronic standards (<100 Hz), the possible implications of a bistable molecular switch are profound. The on/off conductance ratio and cycle lifetime varied for different molecular structures, and were interpreted in the context of the donor−acceptor behavior underlying molecular rectifiers.[201]

Although the concept of a molecular switch generated considerable excitement, uncertainty arose about the mechanism. The possibility that metal filaments might form under high electric fields was considered as an alternative switching mechanism which does not directly involve the molecular monolayer.[198,206] If a metallic short circuit were alternately formed and broken during potential scanning, the *i*/*V* curve of Figure 27 might result. Reconstruction of gold STM tips has been

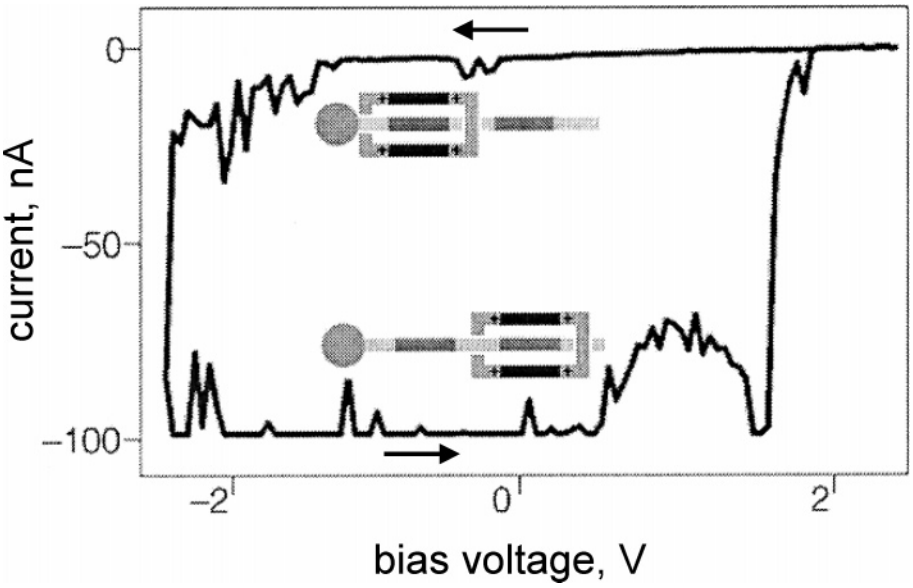

Figure 27. Current/voltage curve of a pseudorotaxane monolayer in an LB molecular junction, showing hysteresis and bistable conductivity. Reprinted from ref 92. Copyright 2001 American Chemical Society.

reported in response to an applied electric field,[173] and metal filaments have been reported for LB rectifiers under certain conditions.[198] The formation of metal filaments may be weakly dependent on the molecular structure in the junction, and represents a serious artifact if present. The observation of conductance switching in metal/molecule/metal junctions based on both rotaxane and alkane molecules resulted in the conclusion that the observed switching was controlled by properties of the metal/molecule interface rather than the molecule itself.[207]

6. Irreversibly Bonded Molecular Junctions

As noted in section 2.2, a third class of molecular junctions based on Si−C, Si−O−C, and C−C bonds may be added to the much larger groups of LB and SAM structures. The term "irreversibly bonded" is not meant to necessarily imply fundamental differences from LB and SAM junctions, but it does serve as a label which indicates strong, covalent bonding between a molecular layer and at least one contact. Three examples were shown in Figure 6, for the case of olefin addition to Si(001), Si−O−C bonding on Si, and C−C bonding on sp^2-hybridized carbon. The Si−O−C linkage was the basis of the redox storage junction already discussed in section 4.1. The Si−C and C−C cases have been investigated in molecular junctions in single-molecule and monolayer junctions, respectively.

6.1. Irreversibly Bonded Junctions on Silicon. The Hamers group has extensively investigated covalent bonding by olefin cycloaddition to silicon[107,108,110,115,208−214] and diamond.[109,208,215] The Si(001) surface has Si=Si double bonds in an ordered array when prepared in UHV. Cycloaddition of olefins to these bonds results in two covalent Si−C bonds. XPS, FTIR, and STM were used to provide a detailed structural model for the resulting surface, and the cycloaddition mechanism was reported. An STM image of cyclopentene chemisorbed to Si(100) showed that the tunneling barrier was reduced when the tip was positioned over an adsorbed molecule.[209] Conjugated adsorbates were also examined, and the importance of π conjugation to the addition reaction was investigated.[108,115] The STM studies of Si/adsorbate surfaces are analogous to those of Au/SAM surfaces described in section 3.1, but without the second covalent bond provided by a dithiol.

Wang et al. have reported silicon/molecule/metal junctions based on covalent bonding to silicon via diazonium ion reduction.[216] A Ti/Au top contact completed the junction, and nonlinear current/voltage curves were observed for 6−32% of the finished junctions. The current was weakly dependent on temperature, leading the authors to conclude that the dominant ET mechanism was tunneling rather than a thermally activated process such as Schottky emission. An alternative silicon-based junction design was investigated by Liu and Yu, consisting of a Hg drop top contact on a alkane monolayer bonded to silicon via a Grignard reaction.[217] The junctions were modeled as modified semiconductor/metal Schottky diodes, and the ET behavior was examined as a function of alkyl chain length. The relatively low β of 0.63 per CH_2 unit was attributed to lower density packing of alkanes and Si compared to metals. Given the importance of silicon in microelectronics, and the stability of the Si−C bond, molecular junctions based on Si substrates are likely to become more common.

6.2. Carbon-Based Molecular Junctions. Covalent bonding of organic molecules to carbon, silicon, and metals via reduction of diazonium reagents has been studied extensively. In most cases, the diazonium reagent is reduced electrochemically from solution, to yield a phenyl radical.[112−114,218−222] Since the reactive radical is formed at the conducting surface, it may rapidly bond to the substrate to form a densely packed mono- or multilayer. The strong Si−C or C−C surface bond forms irreversibly, so no annealing or restructuring has been observed following chemisorption. Modification layers formed by diazonium reduction have been characterized by XPS, STM, AFM, Raman, FTIR, ellipsometry, etc, and the relevant reactions are shown in Figure 28. Chemisorption has been shown to occur

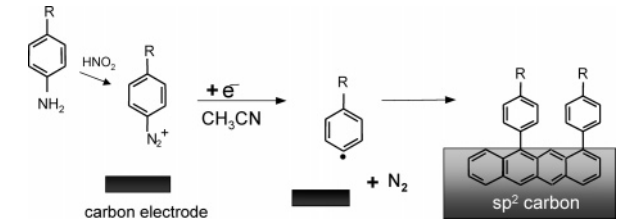

Figure 28. Covalent bonding to carbon surfaces by reduction of diazonium ions in acetonitrile. After synthesis from an aromatic amine, the diazonium reagent is dissolved in acetonitrile or dilute aqueous acid. Phenyl radical may add to either an unsatisfied valence on the carbon surface or to double bonds in the graphitic substrate.

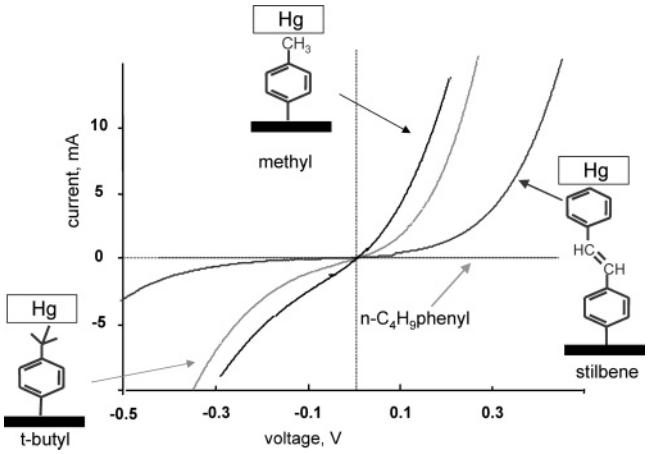

Figure 29. Current/voltage curves for 0.0078 cm^2 junctions formed by lowering a Hg drop onto monolayers on carbon substrates. The labels refer to the diazonium reagent used to form the monolayer, in all cases derivatives of phenyldiazonium tetrafluoroborate. Adapted from ref 190.

spontaneously without an applied potential, via electron transfer from the substrate to the diazonium reagent.[223,224] Although diazonium ions are not particularly strong oxidizing agents, the irreversibility of their reductions drives electron transfer from a conducting or semiconducting surface. The resulting C−C and Si−C bonds are quite stable, but formation is not self-limiting as with thiols, so care is required to control and verify the layer thickness. A brief discussion of a Au/molecule/STM junction based on diazonium reduction appeared in 2002,[132] but the majority of diazonium-based molecular junctions have been on carbon substrates.

6.2.1. Carbon/Molecule/Hg Junctions. Very flat sp^2-hybridized carbon surfaces (rms roughness <5 Å) may be prepared by pyrolysis of photoresist materials in a hydrogen-containing atmosphere.[225,226] After modification by diazonium reduction, a top contact was made with a pendent Hg drop.[190−192] Figure 29 shows *i/V* curves for junctions made from several diazonium reagents with different lengths. The observed conductance was strongly dependent on the monolayer thickness, and was significantly higher for conjugated structures (e.g., stilbene) compared to aliphatic structures. A detailed study of carbon/terphenyl/Hg junction conductance as a function of temperature showed an activated region above 0 °C and a *T*-independent region at lower temperature.[191] This behavior was interpreted as a transition from a tunneling mechanism at low *T* to hopping or thermionic emission at high *T*. The room temperature resistance of such junctions varied strongly

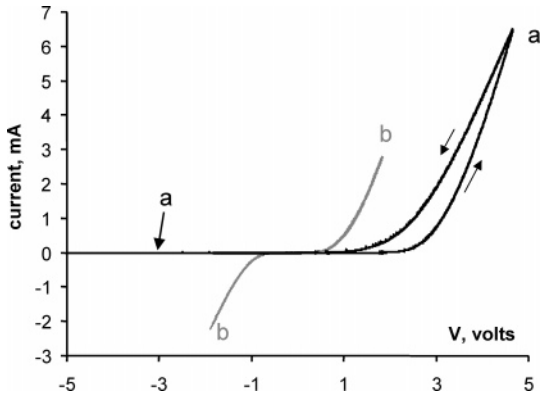

Figure 30. Current/voltage curves of carbon/nitroazobenzene/Ti/Au junctions, with a 3.7 nm thick NAB layer (1 V/s, room temperature, junction area of 0.00196 cm^2). For curve a, Ti was deposited at 0.03 nm/s with a back pressure of 8×10^{-6} Torr. For curve b, Ti was deposited at 0.1 nm/s with a back pressure of 4×10^{-7} Torr. Adapted from ref 227.

with molecule length, being 34 Ω, 13.8 kΩ, and 41.0 kΩ for phenyl, biphenyl, and terphenyl, respectively.

6.2.2. Carbon/Molecule/Titanium Junctions. The carbon/molecule surfaces described in section 6.2.1 have been used to make a molecular junction with vapor-deposited titanium followed by a protective layer of Au. Although Ti is considered a reactive metal (section 4.2) capable of destroying SAMs on Au,[176−178] Raman spectroscopy showed that Ti reacted with the nitro group on a nitroazobenzene monolayer on carbon, but did not significantly affect the remaining monolayer structure.[224] XPS showed a Ti−N bond, implying that Ti deposition on carbon modified with NAB resulted in a carbon/NAB/Ti junction with covalent contacts at both interfaces. The *i/V* curve for such a junction with a 37 Å NAB multilayer is shown in Figure 30a.[227] The junction is strongly rectifying, and shows hysteresis when scanned at 1 V/s at room temperature. The hysteresis was temperature and scan rate dependent, and the transition from a low-conductance state to a high-conductance state was faster for larger applied voltage. The thermally activated, potential-dependent nature of the transition led to the conclusion that the process was a redox reaction driven by the applied field, probably involving rehybridization of the nitroazobenzene structure.[192,227]

Subsequent experiments showed that the hysteresis and rectification were strongly dependent on trace gases present during Ti deposition.[228] Upon reduction of the back pressure by a factor of 20, the *i/V* curve of Figure 30b resulted. The junction resistance was significantly lower, and the rectification and hysteresis were absent. The presence of titanium(II) and titanium(III) oxides revealed by XPS depth profiling indicated that the original deposition conditions produced a Ti film which was partially oxidized. The details are currently under investigation, but it appears that the behavior of Figure 30b is at least partly a result of redox reactions in the Ti/TiO_x and/or NAB films in the carbon/NAB/Ti/Au junction.

7. Issues and Challenges

Although the characteristics of molecular electronic junctions are only beginning to emerge, some conceptual

and technical challenges are already apparent. The list below is certainly not comprehensive, and undoubtedly additional issues will arise as junction properties are understood. Nevertheless, it is useful to consider a few of the many technical challenges posed by investigations of molecular junction behavior.

First, the persistent problem of avoiding defects and short circuits is a major roadblock to reproducible results. When junction behavior is unknown and/or hard to predict, defects can be very misleading. On the practical side, it is likely a large number of molecular junctions (i.e., 10^2-10^7) will be required to perform a useful microelectronic task, e.g., memory or processing. It will be necessary to devise methods for massively parallel fabrication, either with near-perfect yield or with fault-tolerant architecture or software.

Second, the search for a low-barrier ohmic contact between a conductor and a molecule is far from complete. Most currently used interfaces have significant barriers to electron injection, which can dominate junction behavior.

Third, the alignment of the Fermi levels of the contact with the energy levels in the molecule is generally unknown, as is the electric field distribution through the junction. The energy of the HOMO and LUMO relative to the contact Fermi level(s) determines the electron transport barrier in many situations, yet this important parameter is difficult to determine. Furthermore, the HOMO and LUMO energies both vary with their position in the imposed electric field (Figure 10). Generally, it is not known if the highest fields are at the molecule/contact interface(s) or within the molecular layer.

Fourth, lateral interactions between molecules in multiple-molecule junctions are likely, and may be difficult to model. Such interactions may be electrostatic, such as a Coulombic barrier caused by electron transfer to an adjacent molecule, or they may result in orbital mixing and energy splittings from intermolecular interactions. Lateral interactions will affect the "scaling laws" that apply when a single-molecule observation is extended to a possibly large collection of molecules in a monolayer junction.

Finally, realization of useful electronic devices based on molecular junctions will require a combination of empirical characterization of particular junctions with a sophisticated application of theoretical approaches to electron transport. By analogy to conventional microelectronics, we need to determine how molecular components may be combined to realize useful electronic functions.[5] Such a "rational design" of molecular electronic devices will presumably be based on a set of "rules" on how molecules behave as circuit components, combined with quantum mechanical modeling of molecular or supermolecular components. Although the theoretical and practical barriers to designing molecular circuits may be formidable, the large number of degrees of freedom in molecular structures yield vast flexibility in how molecular electronic devices may be exploited. Much of the driving force for understanding molecular junctions stems from possible applications in microelectronics, chemical and biological sensing, and the realm of photonics and the photonic/electronic interface.

Acknowledgment. Preparation of this review and the work discussed from my laboratory were supported by the Analytical and Surface Chemistry Division of the National Science Foundation and by ZettaCore, Inc.

References

(1) Mirkin, C. A.; Ratner, M. A. *Annu. Rev. Phys. Chem.* **1992**, *43*, 719.
(2) Datta, S. *ElectronicTransport in Mesoscopic Systems*; Cambridge University Press: Cambridge, U.K., 1995.
(3) Jortner, J.; Ratner, M. *Molecular Electronics*; Blackwell Science Ltd.: Oxford, U.K., 1997.
(4) Heath, J. R.; Ratner, M. A. *Phys. Today* **2003**, *56*, 43.
(5) Joachim, C.; Gimzewski, J. K.; Aviram, A. *Nature* **2000**, *408*, 541.
(6) Davis, W. B.; Svec, W. A.; Ratner, M. A.; Wasielewski, M. R. *Nature* **1998**, *396*, 60.
(7) Schwab, P. F. H.; Levin, M. D.; Michl, J. *Chem. Rev.* **1999**, *99*, 1863.
(8) Helms, A.; Heller, D.; McLendon, G. *J. Am. Chem. Soc.* **1992**, *114*, 6227.
(9) Hayes, R. T.; Walsh, C. J.; Wasielewski, M. R. *J. Phys. Chem. A* **2004**, *108*, 2375.
(10) Lewis, F. D.; Liu, J.; Zuo, X.; Hayes, R. T.; Wasielewski, M. R. *J. Am. Chem. Soc.* **2003**, *125*, 4850.
(11) Segal, D.; Nitzan, A.; Davis, W. B.; Wasielewski, M. R.; Ratner, M. A. *J. Phys. Chem. B* **2000**, *104*, 3817.
(12) Weiss, E. A.; Ratner, M. A.; Wasielewski, M. R. *J. Phys. Chem. A* **2003**, *107*, 3639.
(13) Sikes, H. D.; Smalley, J. F.; Dudek, S. P.; Cook, A. R.; Newton, M. D.; Chidsey, C. E. D.; Feldberg, S. W. *Science* **2001**, *291*, 1519.
(14) Li, J.; Schuler, K.; Creager, S. E. *J. Electrochem. Soc.* **2000**, *147*, 4584.
(15) Creager, S.; Yu, C. J.; Bamdad, C.; O'Connor, S.; MacLean, T.; Lam, E.; Chong, Y.; Olsen, G. T.; Luo, J.; Gozin, M.; Kayyem, J. F. *J. Am. Chem. Soc.* **1999**, *121*, 1059.
(16) Weber, K.; Hockett, L.; Creager, S. *J. Phys. Chem. B* **1997**, *101*, 8286.
(17) Richardson, J. N.; Peck, S. R.; Curtin, L. S.; Tender, L. M.; Terrill, R. H.; Carter, M. T.; Murray, R. W.; Rowe, G. K.; Creager, S. E. *J. Phys. Chem.* **1995**, *99*, 766.
(18) Sachs, S. B.; Dudek, S. P.; Hsung, R. P.; Sita, L. R.; Smalley, J. F.; Newton, M. D.; Feldberg, S. W.; Chidsey, C. E. D. *J. Am. Chem. Soc.* **1997**, *119*, 10563.
(19) Smalley, J. F.; Feldberg, S. W.; Chidsey, C. E. D.; Linford, M. R.; Newton, M. D.; Liu, Y.-P. *J. Phys. Chem.* **1995**, *99*, 13141.
(20) Chidsey, C. E. D. *Science* **1991**, *251*, 919.
(21) Sumner, J. J.; Weber, K. S.; Hockett, L. A.; Creager, S. E. *J. Phys. Chem.* **2000**, *104*, 7449.
(22) Terrill, R. H.; Murray, R. W. Electron Hopping Transport in Electrochemically Active, Molecular Mixed Valent Materials. In *Molecular Electronics*; Jortner, J., Ratner, M., Eds.; Blackwell Science Ltd.: Oxford, U.K., 1997; p 215.
(23) Chidsey, C. E. D.; Murray, R. W. *Science* **1986**, *231*, 25.
(24) Geng, L.; Reed, R. A.; Kim, M.-H.; Wooster, T. T.; Oliver, B. N.; Egekeze, J.; Kennedy, R. T.; Jorgenson, J. W.; Parcher, J. F.; Murray, R. W. *J. Am. Chem. Soc.* **1989**, *111*, 1614.
(25) Leidner, C. R.; Murray, R. W. *J. Am. Chem. Soc.* **1985**, *107*, 556.
(26) McCarley, R. L.; Thomas, R. E.; Irene, E. A.; Murray, R. W. *J. Electrochem. Soc.* **1990**, *137*, 1485.
(27) McCarley, R. L.; Thomas, R. E.; Irene, E. A.; Murray, R. W. *J. Electroanal. Chem.* **1990**, *290*, 79.
(28) Hutchison, G. R.; Zhao, Y.-J.; Delley, B.; Freeman, A. J.; Ratner, M. A.; Marks, T. J. *Phys. Rev. B* **2003**, *68*, 035204/1.
(29) Mujica, V.; Kemp, M.; Roitberg, A.; Ratner, M. *J. Chem. Phys.* **1996**, *104*, 7296.
(30) Segal, D.; Nitzan, A.; Ratner, M.; Davis, W. D. *J. Phys. Chem. B* **2000**, *104*, 2790.
(31) Yaliraki, S. N.; Ratner, M. A. *J. Phys. Chem.* **1998**, *109*, 5036.
(32) Yaliraki, S. N.; Kemp, M.; Ratner, M. A. *J. Am. Chem. Soc.* **1999**, *121*, 3428.
(33) Yaliraki, S. N.; Roitberg, A. E.; Gonzalez, C.; Mujica, V.; Ratner, M. A. *J. Phys. Chem.* **1999**, *111*, 6997.
(34) Di Ventra, M.; Kim, S.-G.; Pantelides, S. T.; Lang, N. D. *Phys. Rev. Lett.* **2001**, *86*, 288.
(35) Pantelides, S. T.; DiVentra, M.; Lang, N. D. *Physica B* **2001**, *296*, 72.
(36) Di Ventra, M.; Pantelides, S. T.; Lang, N. D. *Phys. Rev. Lett.* **2000**, *84*, 979.
(37) Aviram, A.; Ratner, M. *Chem. Phys. Lett.* **1974**, *29*, 277.
(38) Weidkamp, K. P.; Hacker, C. A.; Schwartz, M. P.; Cao, X.; Tromp, R. M.; Hamers, R. J. *J. Phys. Chem. B* **2003**, *107*, 11142.
(39) Babel, A.; Jenekhe, S. A. *J. Am. Chem. Soc.* **2003**, *125*, 13656.
(40) Burgi, L.; Friend, R. H.; Sirringhaus, H. *Appl. Phys. Lett.* **2003**, *82*, 1482.

(41) Burroughes, J. H.; Jones, C. A.; Friend, R. H. *Nature* **1988**, *335*, 137.
(42) Javey, A.; Guo, J.; Farmer, D. B.; Wang, Q.; Wang, D.; Gordon, R. G.; Lundstrom, M.; Dai, H. *Langmuir* **2004**, *4*, 447.
(43) Meijer, E. J.; Matters, M.; Herwig, P. T.; de Leeuw, D. M.; Klapwijk, T. M. *Appl. Phys. Lett.* **2000**, *76*, 3433.
(44) Mushrush, M.; Facchetti, A.; Lefenfeld, M.; Katz, H. E.; Marks, T. J. *J. Am. Chem. Soc.* **2003**, *125*, 9414.
(45) Collins, P. G.; Bradley, K.; Ishigami, M.; Zettl, A. *Science* **2000**, *287*, 1801.
(46) Diehl, M. R.; Steuerman, D. W.; Tseng, H.-r.; Vignon, S. A.; Star, A.; Celestre, P. C.; Stoddart, J. F.; Heath, J. R. *ChemPhysChem.* **2003**, *4*, 1335.
(47) Fagas, G.; Cuniberti, G.; Richter, K. *Phys. Rev. B: Condens. Matter Mater. Phys.* **2001**, *63*, 045416/1.
(48) Farajian, A. A.; Yakobson, B. I.; Mizuseki, H.; Kawazoe, Y. *Phys. Rev. B* **2003**, *67*, 205423.
(49) Li, H.; Zhou, B.; Lin, Y.; Gu, L.; Wang, W.; Fernando, K. A. S.; Kumar, S.; Allard, L. F.; Sun, Y.-P. *J. Am. Chem. Soc.* **2004**, *126*, 1014.
(50) Peng, H.; Alemany, L. B.; Margrave, J. L.; Khabashesku, V. N. *J. Am. Chem. Soc.* **2003**, *125*, 15174.
(51) Rueckes, T.; Kim, K.; Joselevich, E.; Tseng, G. Y.; Cheung, C.; Lieber, C. M. *Science* **2000**, *289*, 94.
(52) Tans, S. J.; Devoret, M. H.; Dai, H.; Thess, A.; Smalley, R. E.; Geerligs, L. J.; Dekker, C. *Nature* **1997**, *386*, 474.
(53) Xue, Y.; Ratner, M. A. *Phys. Rev. B* **2003**, *68*, 115406.
(54) Xue, Y.; Ratner, M. A. *Phys. Rev. B* **2003**, *68*, 115407.
(55) Burin, A. L.; Ratner, M. A. *J. Phys. Chem.* **2000**, *113*, 3941.
(56) Nitzan, A.; Ratner, M. A. *Science* **2003**, *300*, 1384.
(57) Lamb, D. R. *Electrical Conduction Mechanisms in Thin Insulating Films*; Methuen and Co.: London, 1968.
(58) Simmons, J. G. *DC Conduction in Thin Films*; Mills and Boon Ltd.: London, 1971.
(59) Wold, D. J.; Frisbie, C. D. *J. Am. Chem. Soc.* **2001**, *123*, 5549.
(60) Slowinski, K.; Slowinska, K. U.; Majda, M. *J. Phys. Chem. B* **1999**, *103*, 8544.
(61) Holmlin, R. E.; Haag, R.; Chabinyc, M. L.; Ismagilov, R. F.; Cohen, A. E.; Terfort, A.; Rampi, M. A.; Whitesides, G. M. *J. Am. Chem. Soc.* **2001**, *123*, 5075.
(62) Yamamoto, H.; Waldeck, D. H. *J. Phys. Chem. B* **2002**, *106*, 7469.
(63) Newton, M. D. *Theor. Chem. Acc.* **2003**, *110*, 307.
(64) Skourtis, S. S.; Archontis, G.; Xie, Q. *J. Chem. Phys.* **2001**, *115*, 9444.
(65) Li, X.-Q.; Zhang, H.; Yan, Y. *J. Phys. Chem. A* **2001**, *105*, 9563.
(66) Nitzan, A.; Jortner, J.; Wilkie, J.; Burin, A. L.; Ratner, M. A. *J. Phys. Chem. B* **2000**, *104*, 5661.
(67) Abu-Hilu, M.; Peskin, U. *Chem. Phys.* **2004**, *296*, 231.
(68) Galperin, M.; Segal, D.; Nitzan, A. *J. Chem. Phys.* **1999**, *111*, 1569.
(69) Selzer, Y.; Cabassi, M. A.; Mayer, T. S.; Allara, D. L. *J. Am. Chem. Soc.* **2004**, *126*, 4052.
(70) Murphy, C. J.; Arkin, M. R.; Jenkins, Y.; Ghatlia, N. D.; Bossmann, S. H.; Turro, N. J.; Barton, J. K. *Science* **1993**, *262*, 1025.
(71) O'Neill, M. A.; Dohno, C.; Barton, J. K. *J. Am. Chem. Soc.* **2004**, *126*, 1316.
(72) Hall, D. B.; Barton, J. K. *J. Am. Chem. Soc.* **1997**, *119*, 5045.
(73) Holmlin, R. E.; Dandliker, P. J.; Barton, J. K. *Angew. Chem., Int. Ed. Engl.* **1997**, *36*, 2715.
(74) Zhang, H.; Li, X.-Q.; Han, P.; Yu, X. Y.; Yan, Y. *J. Chem. Phys.* **2002**, *117*, 4578.
(75) Grozema, F. C.; Berlin, Y. A.; Siebbeles, L. D. A. *J. Am. Chem. Soc.* **2000**, *122*, 10903.
(76) Mujica, V.; Roitberg, A. E.; Ratner, M. A. *J. Phys. Chem.* **2000**, *112*, 6834.
(77) Mujica, V.; Ratner, M. A. *Chem. Phys.* **2001**, *264*, 365.
(78) Berlin, Y. A.; Hutchison, G. R.; Rempala, P.; Ratner, M. A.; Michl, J. *J. Phys. Chem. A* **2003**, *107*, 3970.
(79) Bixon, M.; Jortner, J. *J. Am. Chem. Soc.* **2001**, *123*, 12556.
(80) Bixon, M.; Jortner, J. *J. Phys. Chem. A* **2001**, *105*, 10322.
(81) Renger, T.; Marcus, R. A. *J. Phys. Chem. A* **2003**, *107*, 8404.
(82) Hutchison, G. R.; Ratner, M. A.; Marks, T. J.; Naaman, R. *J. Phys. Chem. B* **2001**, *105*, 2881.
(83) Magoga, M.; Joachim, C. *Phys. Rev. B* **1999**, *59*, 16011.
(84) Joachim, C. *Superlattices Microstruct.* **2000**, *28*, 305.
(85) Sze, S. M. *The Physics of Semiconductor Devices*, 2nd ed.; Wiley: New York, 1981.
(86) Zhou, C.; Deshpande, M. R.; Reed, M. A.; Jones, L.; Tour, J. M. *Appl. Phys. Lett.* **1997**, *71*, 611.
(87) Metzger, R. M.; Xu, T.; Peterson, I. R. *J. Phys. Chem. B* **2001**, *105*, 7280.
(88) Metzger, R. M.; Chen, B.; Hopfner, U.; Lakshmikantham, M. V.; Vuillaume, D.; Kawai, T.; Wu, X.; Tachibana, H.; Hughes, T. V.; Sakurai, H.; Baldwin, J. W.; Hosch, C.; Cava, M. P.; Brehmer, L.; Ashwell, G. J. *J. Am. Chem. Soc.* **1997**, *119*, 10455.
(89) Wong, E. W.; Collier, C. P.; Behloradsky, M.; Raymo, F. M.; Stoddart, J. F.; Heath, J. R. *J. Am. Chem. Soc.* **2000**, *122*, 5831.
(90) Collier, C. P.; Wong, E. W.; Belohradsky, M.; Raymo, F. M.; Stoddart, J. F.; Kuekes, P. J.; Williams, R. S.; Heath, J. R. *Science* **1999**, *285*, 391.
(91) Metzger, R. M. *Chem. Rev.* **2003**, *103*, 3803.
(92) Pease, A. R.; Jeppesen, J. O.; Stoddart, J. F.; Luo, Y.; Collier, C. P.; Heath, J. R. *Acc. Chem. Res.* **2001**, *34*, 433.
(93) Finklea, H. O.; Hanshew, D. D. *J. Am. Chem. Soc.* **1992**, *114*, 3173.
(94) Garcias, D. H.; Tein, J.; Breen, T. L.; Hsu, C.; Whitesides, G. M. *Science* **2000**, *289*, 1170.
(95) Porter, M. D.; Bright, T. B.; Allara, D. L.; Chidsey, C. E. D. *J. Am. Chem. Soc.* **1987**, *109*, 3559.
(96) Hooper, A.; Fisher, G. L.; Konstadinidis, K.; Jung, D.; Nguyen, H.; Opila, R.; Collins, R. W.; Winograd, N.; Allara, D. L. *J. Am. Chem. Soc.* **1999**, *121*, 8052.
(97) Fisher, G. L.; Hooper, A.; Opila, R. L.; Jung, D. R.; Allara, D. L.; Winograd, N. *J. Electron Spectrosc. Relat. Phenom.* **1999**, *98*−*99*, 139.
(98) Bumm, L. A.; Arnold, J. J.; Dunbar, T. D.; Allara, D. L.; Weiss, P. S. *J. Phys. Chem.* **1999**, *103*, 8122.
(99) Xue, Y.; Datta, S.; Hong, S.; Reifenberger, R.; Henderson, J. I.; Kubiak, C. P. *Phys. Rev. B* **1999**, *59*, R7852.
(100) Stapleton, J. J.; Harder, P.; Daniel, T. A.; Reinard, M. D.; Yao, Y.; Price, D. W.; Tour, J. M.; Allara, D. L. *Langmuir* **2003**, *19*, 8245.
(101) Gryko, D. T.; Zhao, F.; Yasseri, A. A.; Roth, K. M.; Bocian, D. F.; Kuhr, W. G.; Lindsey, J. S. *J. Org. Chem.* **2000**, *65*, 7356.
(102) Gryko, D. T.; Clausen, C.; Roth, K. M.; Dontha, N.; Bocian, D. F.; Kuhr, W. G.; Lindsey, J. S. *J. Org. Chem.* **2000**, *65*, 7345.
(103) Finklea, H. O. Electrochemistry of Organized Monolayers of Thiols and Related Molecules on Electrodes. In *Electroanalytical Chemistry*; Bard, A. J., Ed.; Dekker: New York, 1996; Vol. 19, p 109.
(104) Smalley, J. F.; Finkea, H. O.; Chidsey, C. E. D.; Linford, M. R.; Creager, S. E.; Ferraris, J. P.; Chalfant, K.; Zawodzinsk, T.; Feldberg, S. W.; Newton, M. D. *J. Am. Chem. Soc.* **2003**, *125*, 2004.
(105) Holten, D.; Bocian, D. F.; Lindsey, J. S. *Acc. Chem. Res.* **2002**, *35*, 57.
(106) Liu, Z.; Yasseri, A. A.; Lindsey, J. S.; Bocian, D. F. *Science* **2003**, *302*, 1543.
(107) Hamers, R. J.; Coulter, S. K.; Ellison, M. D.; Hovis, J. S.; Padowitz, D. F.; Schwartz, M. P.; Greenlief, C. M.; Russell, J. N., Jr. *Acc. Chem. Res.* **2000**, *33*, 617.
(108) Schwartz, M. P.; Hamers, R. J. *Surf. Sci.* **2002**, *515*, 75.
(109) Knickerbocker, T.; Strother, T.; Schwartz, M. P.; Russell, J. N., Jr.; Butler, J.; Smith, L. M.; Hamers, R. J. *Langmuir* **2003**, *19*, 1938.
(110) Cai, W.; Lin, Z.; Strother, T.; Smith, L. M.; Hamers, R. J. *J. Phys. Chem. B* **2002**, *106*, 2656.
(111) de Villeneuve, C. H.; Pinson, J.; Bernard, M. C.; Allongue, P. *J. Phys. Chem. B* **1997**, *101*, 2415.
(112) Allongue, P.; Delamar, M.; Desbat, B.; Fagebaume, O.; Hitmi, R.; Pinson, J.; Saveant, J. M. *J. Am. Chem. Soc.* **1997**, *119*, 201.
(113) Delamar, M.; Hitmi, R.; Pinson, J.; Saveant, J. M. *J. Am. Chem. Soc.* **1992**, *114*, 5883.
(114) Liu, Y.-C.; McCreery, R. L. *J. Am. Chem. Soc.* **1995**, *117*, 11254.
(115) Fang, L.; Liu, J.; Coulter, S.; Cao, X.; Schwartz, M. P.; Hacker, C.; Hamers, R. J. *Surf. Sci.* **2002**, *514*, 362.
(116) McCarty, G. S.; Weiss, P. S. *Chem. Rev.* **1999**, *99*, 1983.
(117) Andres, R. P.; Bein, T.; Dorogi, M.; Feng, S.; Henderson, J. I.; Kubiak, C. P.; Mahony, W.; Osifchin, R. G.; Reifenberger, R. *Science* **1996**, *272*, 1323.
(118) Datta, S.; Tian, W.; Hong, S.; Reifenberger, R.; Henderson, J. I.; Kubiak, C. P. *Phys. Rev. Lett.* **1997**, *79*, 2530.
(119) Hong, S.; Reifenberger, R.; Tian, W.; Datta, S.; Henderson, J.; Kubiak, C. P. *Superlattices Microstruct.* **2000**, *28*, 289.
(120) Howell, S.; Kuila, D.; Kasibhatla, B.; Kubiak, C. P.; Janes, D.; Reifenberger, R. *Langmuir* **2002**, *18*, 5120.
(121) Kasibhatla, B. S. T.; Labonte, A. P.; Zahid, F.; Reifenberger, R. G.; Datta, S.; Kubiak, C. P. *J. Phys. Chem. B* **2003**, *107*, 12378.
(122) McNally, H.; Janes, D.; Kasibhatla, B.; Kubiak, C. P. *Superlattices Microstruct.* **2002**, *31*, 239.
(123) Tian, W.; Datta, S.; Hong, S.; Reifenberger, R.; Henderson, J. I.; Kubiak, C. P. *J. Chem. Phys.* **1998**, *109*, 2874.
(124) Tao, N. J. *Phys. Rev. Lett.* **1996**, *76*, 4066.
(125) Xu, B.; Tao, N. J. *Science* **2003**, *301*, 1221.
(126) Donhauser, Z. J.; Mantooth, B. A.; Kelly, K. F.; Bumm, L. A.; Monnell, J. D.; Stapleton, J. J.; Price, D. W.; Rawlett, A. M.; Allara, D. L.; Tour, J. M.; Weiss, P. S. *Science* **2001**, *292*, 2303.
(127) Bumm, L. A.; Arnold, J. J.; Cygan, M. T.; Dunbar, T. D.; Burgin, T. P.; Jones, L.; Allara, D. L.; Tour, J. M.; Weiss, P. S. *Science* **1996**, *271*, 1705.
(128) Cygan, M. T.; Dunbar, T. D.; Arnold, J. J.; Bumm, L. A.; Shedlock, N. F.; Burgin, T. P.; Jones, L.; Allara, D. L.; Tour, J. M.; Weiss, P. S. *J. Am. Chem. Soc.* **1998**, *120*, 2721.
(129) Dunbar, T. D.; Cygan, M. T.; Bumm, L. A.; McCarty, G. S.; Burgin, T. P.; Reinerth, W. A.; Jones, L.; Jackiw, J. J.; Tour, J. M.; Weiss, P. S.; Allara, D. L. *J. Phys. Chem. B* **2000**, *104*, 4880.

(130) Wassel, R. A.; Fuierer, R. R.; Kim, N.; Gorman, C. B. *Nano Lett.* **2003**, *3*, 1617.
(131) Ramachandran, G. K.; Hopson, T. J.; Rawlett, A. M.; Nagahara, L. A.; Primak, A.; Lindsay, S. M. *Science* **2003**, *300*, 1413.
(132) Fan, F.-R. F.; Yang, J.; Cai, L. T.; Price, D. W.; Dirk, S. M.; Kosynkin, D.; Yao, Y.; Rawlett, A. M.; Tour, J. M.; Bard, A. J. *J. Am. Chem. Soc.* **2002**, *124*, 5550.
(133) Fan, F.-R. F.; Lai, R. Y.; Cornil, J.; Karzazi, Y.; Brédas, J.-L.; Cai, L.; Cheng, L.; Yao, Y.; Price, D. W. J.; Dirk, S. M.; Tour, J. M.; Bard, A. J. *J. Am. Chem. Soc.* **2004**, *126*, 2568.
(134) Han, W.; Durantini, E. N.; Moore, T. A.; Moore, A. L.; Gust, D.; Rez, P.; Leatherman, G.; Seely, G. R.; Tao, N.; Lindsay, S. M. *J. Phys. Chem. B* **1997**, *101*, 10719.
(135) Scudiero, L.; Barlow, D. E.; Mazur, U.; Hipps, K. W. *J. Am. Chem. Soc.* **2001**, *123*, 4073.
(136) Mazur, U.; Hipps, K. W. *J. Phys. Chem. B* **1999**, *103*, 9721.
(137) Mazur, U.; Hipps, K. W. *J. Phys. Chem.* **1995**, *99*, 6684.
(138) Mazur, U.; Hipps, K. W. *J. Phys. Chem.* **1994**, *98*, 8169.
(139) Song, I. K.; Barteau, M. A. *Langmuir* **2004**, *20*, 1850.
(140) Wassel, R. A.; Credo, G. M.; Fuierer, R. R.; Feldheim, D. L.; Gorman, C. B. *J. Am. Chem. Soc.* **2004**, *126*, 295.
(141) Ashwell, G. J.; Tyrrell, W. D.; Whittam, A. J. *J. Am. Chem. Soc.* **2004**, *126*, 7102.
(142) Rawlett, A. M.; Hopson, T. J.; Nagahara, L. A.; Tsui, R. K.; Ramachandran, G. K.; Lindsay, S. M. *Appl. Phys. Lett.* **2002**, *81*, 3043.
(143) Wold, D. J.; Frisbie, C. D. *J. Am. Chem. Soc.* **2000**, *122*, 2970.
(144) Leatherman, G.; Durantini, E. N.; Gust, D.; Moore, T. A.; Moore, A. L.; Stone, S.; Zhou, Z.; Rez, P.; Li, Y. Z.; Lindsay, S. M. *J. Phys. Chem. B* **1999**, *103*, 4006.
(145) Beebe, J. M.; Engelkes, V. B.; Miller, L. L.; Frisbie, C. D. *J. Am. Chem. Soc.* **2002**, *124*, 11268.
(146) Ramachandran, G. K.; Tomfohr, J. K.; Sankey, O. F.; Li, J.; Zarate, X.; Primak, A.; Terazano, Y.; Moore, T. A.; Moore, A. L.; Gust, D.; Nagahara, L. A.; Lindsay, S. M. *J. Phys. Chem. B* **2003**, *107*.
(147) Cui, X. D.; Primak, A.; Zarate, X.; Tomfohr, J.; Sankey, O. F.; Moore, A. L.; Moore, T. A.; Gust, D.; Nagahara, L. A.; Lindsay, S. M. *J. Phys. Chem. B* **2002**, *106*, 8604.
(148) Lindsay, S. M. *Interface* **2004**, *13*.
(149) Cui, X. D.; Primak, A.; Zarate, X.; Tomfohr, J.; Sankey, O. F.; Moore, A. L.; Moore, T. A.; Gust, D.; Harris, G.; Lindsay, S. M. *Science* **2001**, *294*, 571.
(150) Nazin, G. V.; Qiu, X. H.; Ho, W. *Science* **2003**, *302*, 77.
(151) Holman, M. W.; Liu, R.; Adams, D. M. *J. Am. Chem. Soc.* **2003**, *125*, 12649.
(152) Hoagland, J. J.; Dowdy, J.; Hipps, K. W. *J. Phys. Chem.* **1991**, *95*, 2246.
(153) Hipps, K. W.; Mazur, U. *J. Phys. Chem.* **1994**, *98*, 5824.
(154) Hipps, K. W.; Mazur, U. Inelastic electron tunneling spectroscopy. In *Handbook of Vibrational Spectrosocpy*; John Wiley & Sons Ltd.: Chichester, U.K., 2002; Vol. 4, p 812.
(155) Reed, M. A.; Zhou, C.; Muller, C. J.; Burgin, T. P.; Tour, J. M. *Science* **1997**, *278*, 252.
(156) Chen, J.; Reed, M. A.; Rawlett, A. M.; Tour, J. M. *Science* **1999**, *286*, 1550.
(157) *Molecular Nanoelectronics*; Reed, M. A., Lee, T., Eds.; American Scientific Publishers: Stevenson Ranch, CA, 2003.
(158) Xiao, X.; Xu, B.; Tao, N. J. *Nano Lett.* **2004**, *4*, 267.
(159) Clausen, C.; Gryko, D. T.; Yasseri, A. A.; Diers, J. R.; Bocian, D. F.; Kuhr, W. G.; Lindsey, J. S. *J. Org. Chem.* **2000**, *62*, 7371.
(160) Roth, K. M.; Dontha, N.; Dabke, R. B.; Gryko, D. T.; Clausen, C.; Lindsey, J. S.; Bocian, D. F.; Kuhr, W. G. *J. Vac. Sci. Technol., B* **2000**, *18*, 2359.
(161) Bocian, D. F.; Kuhr, W. G.; Lindsey, J. High-density non-volatile memory device. U.S. Patent 6,657,884, 2003.
(162) Bocian, D. F.; Kuhr, W. G.; Lindsey, J. S. High-density non-volatile memory device. U.S. Patent 6,381,169, 2002.
(163) Kuhr, W. G. *Interface* **2004**, *13*, 34.
(164) Gryko, D. T.; Clausen, P. C.; Roth, K. M.; Bocian, D. F.; Kuhr, W. G.; Lindsey, J. S. High-Density Non-volatile Memory Device Incorporating Thiol-Derivatized Porphyrins. U.S. Patent 6,208,-553, 2001.
(165) Gryko, D. T.; Junzhong, L.; Diers, J. R.; Roth, K. M.; Bocian, D. F.; Kuhr, W. G.; Lindsey, J. S. *J. Mater. Chem.* **2001**, *11*, 1162.
(166) Clausen, C.; Gryko, D. T.; Dabke, R. B.; Dontha, N.; Bocian, D. F.; Kuhr, W. G.; Lindsey, J. S. *J. Org. Chem.* **2000**, *65*, 7363.
(167) Li, Z.; Gryko, D.; Dabke, R. B.; Diers, J. R.; Bocian, D. F.; Kuhr, W. G.; Lindsey, J. S. *J. Org. Chem.* **2000**, *65*, 7379.
(168) Li, Q.; Mathur, G.; Homsi, M.; Surthi, S.; Misra, V.; Malinovskii, V.; Schweikart, K.-H.; Yu, L.; Lindsey, J. S.; Liu, Z.; Dabke, R. B.; Yasseri, A. A.; Bocian, D. F.; Kuhr, W. G. *Appl. Phys. Lett.* **2002**, *81*, 1494.
(169) Roth, K. M.; Gryko, D. T.; Clausen, C.; Li, Z.; Lindsey, J. S.; Kuhr, W. G.; Bocian, D. F. *J. Phys. Chem. B* **2002**, *106*, 8639.
(170) Schweikart, K.-H.; Malinovskii, V. L.; Diers, J. R.; Yasseri, A. A.; Bocian, D. F.; Kuhr, W. G.; Lindsey, J. S. *J. Mater. Chem.* **2002**, *12*, 808.
(171) Roth, K. M.; Yasseri, A. A.; Liu, Z.; Dabke, R. B.; Malinovskii, V.; Schweikart, K.-H.; Yu, L.; Tiznado, H.; Zaera, F.; Lindsey, J. S.; Kuhr, W. G.; Bocian, D. F. *J. Am. Chem. Soc.* **2003**, *125*, 505.
(172) Snyder, S. R.; White, H. S. *J. Electroanal. Chem.* **1995**, *394*, 177.
(173) Schott, J. H.; White, H. S. *Langmuir* **1993**, *9*, 3471.
(174) Fisher, G. L.; Hooper, A. E.; Opila, R. L.; Jung, D. R.; Allara, D. L.; Winograd, N. *J. Phys. Chem. B* **2000**, *104*, 3267.
(175) Fisher, G. L.; Walker, A. V.; Hooper, A. E.; Tighe, T. B.; Bahnck, K. B.; Skriba, H. T.; Reinard, M. D.; Haynie, B. C.; Opila, R. L.; Winograd, N.; Allara, D. L. *J. Am. Chem. Soc.* **2002**, *124*, 5528.
(176) Konstadinidis, K.; Zhang, P.; Opila, R. L.; Allara, D. L. *Surf. Sci.* **1995**, *338*, 300.
(177) Haynie, B. C.; Walker, A. V.; Tighe, T. B.; Allara, D. L.; Winograd, N. *Appl. Surf. Sci.* **2003**, *203−204*, 433.
(178) Boer, B. d.; Frank, M. M.; Chabal, Y. J.; Jiang, W.; Garfunkel, E.; Bao, Z. *Langmuir* **2004**, *20*, 1539.
(179) Chang, S.-C.; Li, Z.; Lau, C. N.; Larade, B.; Williams, R. S. *Appl. Phys. Lett.* **2003**, *83*, 3198.
(180) Reed, M. A.; Tour, J. M. *Sci. Am.* **2000**, 86.
(181) Chen, J.; Calvet, L. C.; Reed, M. A.; Carr, D. W.; Grubisha, D. S.; Bennett, D. W. *Chem. Phys. Lett.* **1999**, *313*, 741.
(182) Chen, J.; Wang, W.; Reed, M. A.; Rawlett, A. M.; Price, D. W.; Tour, J. M. *Appl. Phys. Lett.* **2000**, *77*, 1224.
(183) Reed, M. A.; Chen, J.; Rawlett, A. M.; Price, D. W.; Tour, J. M. *Appl. Phys. Lett.* **2001**, *78*, 3735.
(184) Cai, L. T.; Skulason, H.; Kushmerick, J. G.; Pollack, S. K.; Naciri, J.; Shashidhar, R.; Allara, D. L.; Mallouk, T. E.; Mayer, T. S. *J. Phys. Chem. B*, in press.
(185) Galperin, M.; Nitzan, A.; Sek, S.; Majda, M. *J. Electroanal. Chem.* **2003**, *550−551*, 337.
(186) Slowinski, K.; Majda, M. *J. Electroanal. Chem.* **2000**, *491*, 139.
(187) Slowinski, K.; Fong, H. K. Y.; Majda, M. *J. Am. Chem. Soc.* **1999**, *121*, 7257.
(188) Rampi, M. A.; Whitesides, G. M. *Chem. Phys.* **2002**, *281*, 373.
(189) Haag, R.; Rampi, M. A.; Holmlin, R. E.; Whitesides, G. M. *J. Am. Chem. Soc.* **1999**, *121*, 7895.
(190) Ranganathan, S.; Steidel, I.; Anariba, F.; McCreery, R. L. *Nano Lett.* **2001**, *1*, 491.
(191) Anariba, F.; McCreery, R. L. *J. Phys. Chem. B* **2002**, *106*, 10355.
(192) Solak, A. O.; Ranganathan, S.; Itoh, T.; McCreery, R. L. *Electrochem. Solid State Lett.* **2002**, *5*, E43.
(193) Scheib, S.; Cava, M. P.; Baldwin, J. W.; Metzger, R. M. *J. Org. Chem.* **1998**, *63*.
(194) Vuillame, D.; Chen, B.; Metzger, R. M. *Langmuir* **1999**, *15*, 4011.
(195) Chen, B.; Metzger, R. M. *J. Phys. Chem.* **1999**, *103*, 4447.
(196) Xu, T.; Morris, T. A.; Szulczewski, G. J.; Amaresh, R. R.; Gao, Y.; Street, S. C.; Kispert, L. D.; Metzger, R. M.; Terenziani, F. *J. Phys. Chem. B* **2002**, *106*, 10374.
(197) Jaiswal, A.; Amaresh, R. R.; Lakshmikantham, M. V.; Honciuc, A.; Cava, M. P.; Metzger, R. M. *Langmuir* **2003**, *19*, 9043.
(198) Metzger, R. M.; Baldwin, J. W.; Shumate, W. J.; Peterson, I. R.; Mani, P.; Mankey, G. J.; Morris, T.; Szulczewski, G.; Bosi, S.; Prato, M.; Comito, A.; Rubin, Y. *J. Phys. Chem. B* **2003**, *107*, 1021.
(199) Metzger, R. M. *Interface* **2004**, *13*.
(200) Chen, Y.; Jung, G.-Y.; Ohlberg, D. A. A.; Li, X.; Stewart, D. R.; Jeppesen, J. O.; Nielsen, K. A.; Stoddart, J. F.; Williams, R. S. *Nanotechnology* **2003**, *14*, 462.
(201) Collier, C. P.; Jeppesen, J. O.; Luo, Y.; Perkins, J.; Wong, E. W.; Heath, J. R.; Stoddart, J. F. *J. Am. Chem. Soc.* **2001**, *123*, 12632.
(202) Luo, Y.; Collier, C. P.; Jeppesen, J. O.; Nielsen, K. A.; Delonno, E.; Ho, G.; Perkins, J.; Tseng, H.-R.; Yamamoto, T.; Stoddart, J. F.; Heath, J. R. *ChemPhysChem* **2002**, *3*, 519.
(203) Chen, Y.; Ohlberg, D. A. A.; Li, X.; Stewart, D. R.; Williams, R. S.; Jeppesen, J. O.; Nielsen, K. A.; Stoddart, J. F.; Olynick, D. L.; Anderson, E. *Appl. Phys. Lett.* **2003**, *82*, 1610.
(204) Collier, C. P.; Mattersteig, G.; Wong, E. W.; Luo, Y.; Beverly, K.; Sampaio, J.; Raymo, F. M.; Stoddart, J. F.; Heath, J. R. *Science* **2000**, *289*, 1172.
(205) Heath, J. R.; Collier, C. P.; Mattersteig, G.; Raymo, F. M.; Stoddart, J. F.; Wong, E. Electrically Addressable Volatile Non-Volatile Molecular-Based Switching Devices. U.S. Patent 6,198,-655, 2001.
(206) Service, R. F. *Science* **2003**, *302*, 556.
(207) Stewart, D. R.; Ohlberg, D. A. A.; Beck, P. A.; Chen, Y.; Williams, R. S.; Jeppesen, J. O.; Nielsen, K. A.; Stoddart, J. F. *Nano Lett.* **2004**, *4*, 133.
(208) Yang, W.; Auciello, O.; Butler, J. E.; Cai, W.; Carlisle, J.; Gerbi, J.; Gruen, D.; Knickerbocker, T.; Lasseter, T.; Russell, J. N. J.; Smith, L. M.; Hamers, R. J. *Nat. Mater.* **2002**, *1*, 253.
(209) Padowitz, D. F.; Hamers, R. J. *J. Phys. Chem.* **1998**, *102*, 8541.
(210) Schwartz, M. P.; Ellison, M. D.; Coulter, S. K.; Hovis, J. S.; Hamers, R. J. *J. Am. Chem. Soc.* **2000**, *122*, 8529.
(211) Cao, X.; Coulter, S. K.; Ellison, M. D.; Liu, H.; Liu, J.; Hamers, R. J. *J. Phys. Chem. B* **2001**, *105*, 3759.
(212) Cao, X.; Hamers, R. J. *J. Am. Chem. Soc.* **2001**, *123*, 10988.
(213) Schwartz, M. P.; Halter, R. J.; McMahon, R. J.; Hamers, R. J. *J. Phys. Chem. B* **2003**, *107*, 224.

(214) Hacker, C. A.; Hamers, R. J. *J. Phys. Chem. B* **2003**, *107*, 7689.
(215) Hovis, J. S.; Coulter, S. K.; Hamers, R. J.; D'Evelyn, M. P.; Russell, J. N.; Butler, J. E. *J. Am. Chem. Soc.* **2000**, *122*, 732.
(216) Wang, W.; Lee, T.; Kamdar, M.; Reed, M. A.; Stewart, M. P.; Hwang, J.-J.; Tour, J. M. *Superlattices Microstruct.* **2003**, *33*, 217.
(217) Liu, Y.-J.; Yu, H.-Z. *ChemPhysChem* **2002**, *9*, 799.
(218) Delamar, M.; Desarmot, G.; Fagebaume, O.; Hitmi, R.; Pinson, J.; Saveant, J. *Carbon* **1997**, *35*, 801.
(219) Coulon, E.; Pinson, J.; Bourzat, J.-D.; Commercon, A.; Pulicani, J.-P. *J. Org. Chem.* **2002**, *67*, 8513.
(220) Coulon, E.; Pinson, J.; Bourzat, J.-D.; Commercon, A.; Pulicani, J.-P. *Langmuir* **2002**, *17*, 7102.
(221) Liu, Y.-C.; McCreery, R. L. *Anal. Chem.* **1997**, *69*, 2091.
(222) Anariba, F.; DuVall, S. H.; McCreery, R. L. *Anal. Chem.* **2003**, *75*, 3837.
(223) Stewart, M. P.; Maya, F.; Kosynkin, D. V.; Dirk, S. M.; Stapleton, J. J.; McGuiness, C. L.; Allara, D. L.; Tour, J. M. *J. Am. Chem. Soc.* **2004**, *126*, 370.
(224) Nowak, A. M.; McCreery, R. L. *Anal. Chem.* **2004**, *76*, 1089.
(225) Ranganathan, S.; McCreery, R. L. *Anal. Chem.* **2001**, *73*, 893.
(226) Ranganathan, S.; McCreery, R. L.; Majji, S. M.; Madou, M. *J. Electrochem. Soc.* **2000**, *147*, 277.
(227) McCreery, R. L.; Dieringer, J.; Solak, A. O.; Snyder, B.; Nowak, A.; McGovern, W. R.; DuVall, S. *J. Am. Chem. Soc.* **2003**, *125*, 10748.
(228) McCreery, R.; Dieringer, J.; Solak, A. O.; Snyder, B.; Nowak, A. M.; McGovern, W. R.; DuVall, S. *J. Am. Chem. Soc.* **2004**, *126*, 6200.

CM049517Q